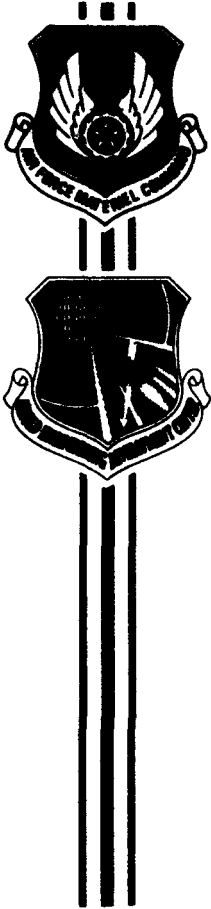


AEDC-TR-93-17

2

AD-A273 671



# Arnold Engineering Development Center Low-Background Blackbody Calibration

C. B. Herron, S. L. Steely, and R. P. Young  
Calspan Corporation/AEDC Operations

November 1993

Final Report for Period February 1990 through June 1993

Approved for public release; distribution is unlimited.

93-30254

**S** DTIC  
ELECTE  
DEC 14 1993  
**A**

**ARNOLD ENGINEERING DEVELOPMENT CENTER  
ARNOLD AIR FORCE BASE, TENNESSEE  
AIR FORCE MATERIEL COMMAND  
UNITED STATES AIR FORCE**

93 12 13 071

## NOTICES

When U. S. Government drawings, specifications, or other data are used for any purpose other than a definitely related Government procurement operation, the Government thereby incurs no responsibility nor any obligation whatsoever, and the fact that the Government may have formulated, furnished, or in any way supplied the said drawings, specifications, or other data, is not to be regarded by implication or otherwise, or in any manner licensing the holder or any other person or corporation, or conveying any rights or permission to manufacture, use, or sell any patented invention that may in any way be related thereto.

Qualified users may obtain copies of this report from the Defense Technical Information Center.

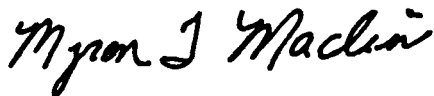
References to named commercial products in this report are not to be considered in any sense as an endorsement of the product by the United States Air Force or the Government.

## DESTRUCTION NOTICE

For unclassified, limited documents, destroy by any method that will prevent disclosure or reconstruction of the document.

## APPROVAL STATEMENT

This report has been reviewed and approved



MYRON T. MACLIN, Major, USAF  
Chief, Flight Dynamics Flight  
Technology Division  
Test Operations Directorate

Approved for publication:

FOR THE COMMANDER



ROBERT T. CROOK  
Director of Technology  
Deputy for Operations

**REPORT DOCUMENTATION PAGE**

Form Approved

OMB No. 0704-0188

Public reporting burden for this collection of information is estimated to average 1 hour per response, including the time for reviewing instructions, searching existing data sources, gathering and maintaining the data needed, and completing and reviewing the collection of information. Send comments regarding this burden estimate or any other aspect of this collection of information, including suggestions for reducing this burden, to Washington Headquarters Services, Directorate for Information Operations and Reports, 1215 Jefferson Davis Highway, Suite 1204, Arlington, VA 22202-4302, and to the Office of Management and Budget, Paperwork Reduction Project (0704-0188), Washington, DC 20503.

1. AGENCY USE ONLY (Leave blank)

2. REPORT DATE

November 1993

3. REPORT TYPE AND DATES COVERED

Final Report - February 1990 through June 1993

4. TITLE AND SUBTITLE

**Arnold Engineering Development Center Low-Background  
Blackbody Calibration**

5. FUNDING NUMBERS

0104

6. AUTHOR(S)

**C. B. Herron, S. L. Steely, and R. P. Young  
Calspan Corporation / AEDC Operations**

7. PERFORMING ORGANIZATION NAME(S) AND ADDRESS(ES)

**Arnold Engineering Development Center / DOT  
Air Force Materiel Command  
Arnold Air Force Base, TN 37389-9011**

8. PERFORMING ORGANIZATION  
(REPORT NUMBER)

AEDC-TR-93-17

9. SPONSORING/MONITORING AGENCY NAMES(S) AND ADDRESS(ES)

10. SPONSORING/MONITORING  
AGENCY REPORT NUMBER

11. SUPPLEMENTARY NOTES

**Available in Defense Technical Information Center (DTIC).**

12a. DISTRIBUTION/AVAILABILITY STATEMENT

**Approved for public release. Distribution is unlimited.**

12b. DISTRIBUTION CODE

13. ABSTRACT (Maximum 200 words)

**Arnold Engineering Development Center low-background, blackbody sources, which emit in the long-wavelength infrared electromagnetic spectrum, have been calibrated at the National Institute of Standards and Technology between 1990 and 1993. These traceable blackbody calibrations have also been transferred to secondary working standards for use in radiometric test facilities. This report provides a summary of the current status and future direction of blackbody calibration at Arnold Engineering Development Center. A complete description of the sources, calibration results, diffraction-correction modeling, and future capabilities is provided.**

14. SUBJECT TERMS

**LWIR  
blackbody**

**radiometrics**

15. NUMBER OF PAGES

72

16. PRICE CODE

17. SECURITY CLASSIFICATION  
OF REPORT  
**UNCLASSIFIED**18. SECURITY CLASSIFICATION  
OF THIS PAGE  
**UNCLASSIFIED**19. SECURITY CLASSIFICATION  
OF ABSTRACT  
**UNCLASSIFIED**20. LIMITATION OF ABSTRACT  
**SAME AS REPORT**

## PREFACE

The work reported herein was performed by the Arnold Engineering Development Center (AEDC), Air Force Materiel Command (AFMC). The results were obtained by Calspan Corporation/AEDC Operations, Aerospace Flight Dynamics support contractor at the AEDC, AFMC, Arnold Air Force Base, TN, under AEDC job number 0104. The Air Force Project Manager is Maj. M. Maclin AEDC/DOTF. This report describes work initiated in February 1990 and completed in June 1993. The manuscript was submitted for publication on October 12, 1993.

Accession For	
NTIS CRA&I	<input checked="" type="checkbox"/>
DTIC TAB	<input type="checkbox"/>
Unannounced	<input type="checkbox"/>
Justification .....	
By .....	
Distribution /	
Availability Codes	
Dist	Avail and/or Special
A-1	

**DTIC QUALITY INSPECTED 3**

## CONTENTS

<b>1.0 INTRODUCTION</b> .....	7
<b>2.0 BLACKBODY PACKAGES</b> .....	7
2.1 Standard Infrared Source IIA .....	7
2.2 Standard Infrared Source IIB .....	8
2.3 Standard Infrared Source III .....	9
2.4 Focal Plane Characterization Chamber Source .....	10
2.5 Transportable Direct Write Scene Generation Source .....	10
2.6 Variable Aperture Blackbody Source .....	11
2.7 Short Wavelength Infrared Source .....	12
<b>3.0 NIST CALIBRATION RESULTS</b> .....	13
3.1 SIRS IIA Calibration .....	14
3.2 SIRS III Calibration .....	15
<b>4.0 AEDC CALIBRATION TRANSFER TECHNIQUE</b> .....	15
4.1 Ultra-High Vacuum Test Chamber .....	16
4.2 IR Labs Bolometer Technique .....	18
4.3 Si:Ga Detector Technique .....	21
<b>5.0 AEDC CALIBRATION TRANSFER RESULTS</b> .....	24
5.1 SIRS IIB Calibration .....	24
5.2 SIRS III Calibration .....	25
5.3 TDWSG Source Calibration .....	26
5.4 VAB Source Calibration .....	27
5.5 SWIR Source Calibration .....	27
<b>6.0 DIFFRACTION CORRECTION MODELING</b> .....	28
<b>7.0 FUTURE CALIBRATION REQUIREMENTS</b> .....	29
<b>8.0 CONCLUDING REMARKS</b> .....	30
REFERENCES .....	30

## ILLUSTRATIONS

<u>Figure</u>	<u>Page</u>
1. Cross-Sectional View of SIRS IIA Assembly .....	33
2. SIRS IIB Blackbody Source .....	34
3. SIRS IIB Assembly .....	35
4. SIRS III Blackbody Core .....	36
5. SIRS III Assembly .....	37
6. FPCC Source Package Installed in the Chamber .....	38
7. TDWSG Source Assembly .....	39

<u>Figure</u>	<u>Page</u>
8. Variable Aperture Blackbody Source (VABS) Assembly .....	40
9. SWIR (1200 K) Blackbody Source .....	41
10. SIRS IIA Installation on NIST Mounting Plate .....	42
11. Hardware Installation in the UHV Chamber .....	43
12. UHV Source Data Acquisition and Control System .....	44
13. Bolometer Dewar System Schematic .....	45
14. Bolometer Responsivity versus Dewar Pressure .....	46
15. Bolometer Instrumentation .....	47
16. Si:Ga Detector Normalized Spectral Response .....	48
17. Si:Ga Detector Responsivity versus Power .....	49
18. SIRS III Transfer Calibration Results, January 1992 .....	50
19. SIRS III Output Linearity .....	51
20. SIRS III Source Evaluation, June 1992 .....	52
21. SWIR Source Output versus Cavity Temperature .....	53

### TABLES

<u>Table</u>	<u>Page</u>
1. SIRS IIA Output Aperture Diameters (Inches) .....	54
2. SIRS IIB Output Aperture Diameters (Inches) .....	54
3. SIRS III Output Aperture Diameters (Inches) .....	55
4. FPCC Source Output Aperture Diameters (Inches) .....	56
5. TDWSG Source Output Aperture Diameters (Inches) .....	56
6. VABS Output Aperture Diameters (Inches) .....	57
7. FY90 SIRS IIA Calibration Equations and Coefficients .....	57
8. FY90 SIRS IIA Calibration Data—Sensor A Aperture 3 .....	58
9. FY90 and FY93 SIRS IIA Diffraction-Correction Percentages .....	59
10. FY93 SIRS IIA Calibration Equations and Coefficients .....	60
11. FY93 SIRS IIA Calibration Data .....	60
12. FY90 and FY93 SIRS IIA Calibration Coefficient Comparison (Temperature Sensor A) .....	61
13. FY90 and FY93 SIRS IIA NIST Calibration Results Comparison (Aperture No. 3) .....	61
14. FY92 SIRS III Calibration Equations and Coefficients—Sensor A .....	62
15. FY92 SIRS III Calibration Data—Sensor A Aperture 16 .....	63
16. FY92 SIRS III Diffraction Correction Percentages .....	64

<u>Table</u>	<u>Page</u>
17. SIRS IIA and SIRS IIB Comparison Summary (Si:Ga, 12 V Bias, 14.9 K, 4/29/92) .....	65
18. SIRS IIA and SIRS III Comparison Summary (Si:Ga, 12 V Bias, 17.9 K, 6/24/92) .....	66
19. SIRS IIA and TDWSG Comparison Summary (Si:Ga, 12 V Bias, 15 K, 9/9/92) .....	67
20. SIRS IIA and VABS Comparison Summary .....	68
21. SWIR Source Calibration Results .....	69

## **1.0 INTRODUCTION**

Earth orbiting satellite-based optical sensors operate in a vacuum environment and detect and discriminate targets against a very low infrared (IR) background. Sensor ground-based test and evaluation (T&E) is performed from the focal plane array (FPA) level of the sensor up to the entire sensor system which includes electronics and optics. Calibration and characterization of sensors is normally accomplished in vacuum chambers having optically tight, cryogenically cooled (20 K) liners which simulate the space environment. Blackbody sources are provided in these chambers to characterize the sensor response to the emitted IR radiation. The IR blackbody sources used in these facilities are generally conical cavities with a small circular output aperture. The source radiant intensity is defined by the cavity temperature and the aperture area.

The calibration traceability of blackbody sources is an important requirement and technology issue for support of IR space sensor testing. A major contributor to the uncertainty of a flight sensor calibration is the calibration of the chamber blackbody sources. AEDC's low-temperature blackbody sources (100 to 400 K) were calibrated at the National Bureau of Standards (NBS) through mid-1984. At this time NBS closed their calibration facility, and AEDC source calibrations were obtained by transfer from a source traceable to the NBS (from an earlier NBS calibration). In late 1989, the National Institute of Standards and Technology (NIST) Low-Background IR (LBIR) facility came on line to replace the former NBS capability. AEDC has worked with NIST since that time to calibrate and re-establish blackbody traceability to the NIST standard.

This report provides a description of the IR blackbody sources presently in use at AEDC. Two of the AEDC standard infrared sources (SIRS IIA and SIRS III) have been calibrated at NIST. Either of these secondary standard sources can be used to calibrate other blackbody sources at AEDC. However, SIRS IIA has a longer traceable history to NIST and is the source generally used to calibrate other sources. Blackbody source calibration is accomplished in the AEDC Ultra-High Vacuum (UHV) Chamber. A description of this facility is included in this report. The purpose of this report is to present the results of recent NIST calibrations of SIRS IIA and SIRS III and to document the results of tests to transfer the NIST calibrations to other AEDC sources.

## **2.0 BLACKBODY PACKAGES**

### **2.1 STANDARD INFRARED SOURCE IIA**

The standard infrared source (SIRS) version IIA is an older blackbody that is used to provide a laboratory standard from which NIST traceability can be transferred to other test

sources. The blackbody core assembly was fabricated at AEDC in 1983. Since then, the core assembly has been integrated with a new multiple aperture housing assembly. A cross-sectional view of the SIRS IIA source assembly is shown in Fig. 1.

The SIRS IIA was designed to operate up to a maximum temperature of 400 K. The blackbody radiator is a re-entrant conical cavity core with an output diameter of 0.177 in. The interior wall of the cavity is anodized to achieve a surface emissivity greater than 0.95. The calculated effective emissivity of the cavity is calculated to be greater than 0.99. The cavity is heated with a platinum wire heater, 0.005-in. diam, wound around the cavity core in a manner that provides uniform core heating. Thermal isolation and mechanical support is accomplished using low-conductivity, thin-wall stainless-steel tubing. The two stainless-steel tubes connect the core mounting arbor to the base mounting flange. This mounting flange is attached to the housing, which normally operates at temperatures below 20 K.

The cavity core is instrumented with two platinum variable resistance temperature sensors that are symmetrically embedded in the heater section near the apex of the cavity. The source temperature is controlled using a Lakeshore feedback-type controller. The Lakeshore controller can maintain cavity temperature to less than  $\pm 0.1$  K. One of the cavity temperature sensors is used as a monitor for the temperature control electronics.

The calibration source is equipped with a 7-position aperture wheel. The aperture wheel contains six precision apertures and one blank position. The aperture diameters for the source are listed in Table 1. Both nominal and measured aperture diameters are provided. The measured value for an aperture was obtained by measuring the diameter every 120 deg and averaging the three values. The standard deviation of these measurements was used as the uncertainty of the diameter measurement. This selection of apertures provides an output dynamic range of nominally 400 in source intensity. All of the apertures are 0.003-in.-thick copper with 0.001-in.-thick electro-formed nickel pinholes, mounted in counter-bored holes. Position of the aperture wheel is controlled by a direct-coupled stepping motor. A rotary potentiometer, connected through a rotary coupling to the rear motor shaft, monitors the aperture wheel angular position. An emitter diode/photo-transistor pair viewing through slits in the aperture wheel also provide an indication of the aperture wheel's position. A cooling strap, connected between the aperture-wheel hub and the source housing, aids in aperture-wheel cooling.

## **2.2 STANDARD INFRARED SOURCE IIB**

The SIRS IIB blackbody, also a laboratory standard source, is illustrated in Fig. 2. Figure 3 is a photograph of the assembly. The SIRS IIB assembly is similar to the SIRS IIA except that it will operate up to 500 K. Table 2 provides the output aperture diameters. Although

the nominal aperture diameters are identical to SIRS IIA, the actual diameters are slightly different as measured.

### 2.3 STANDARD INFRARED SOURCE III

The SIRS III blackbody is the standard infrared source subassembly of the calibration monitoring assembly in the 7V chamber. The source provides multiple intensity outputs (at fixed temperature) for detector linearity measurements. The blackbody radiator is a re-entrant conical cavity core with an output diameter of 0.21 in. Figure 4 is a photograph of the blackbody core. The apex angle of the conical cavity is nominally 18 deg, and the re-entrant section has an angle of 45 deg. The interior wall of the cavity is anodized to achieve a surface emissivity greater than 0.95. The effective emissivity of the cavity is calculated to be greater than 0.99. The source temperature is variable over the range from 150 to 500 K. The cavity is heated with a constantan wire winding, wound around the cavity core in a manner that provides uniform core heating. The heater wire is potted into grooves in the core block. The core block is mounted in a light tight aluminum housing that is conductively cooled from the chamber optical bench. A long conduction path between the heated cavity and the cold core block minimizes heat loss from the cavity core to the surroundings. A stainless-steel shield provides radiation isolation. The core block internal surfaces are also polished to reduce radiation heat loss from the heated core. Less than 2 W are needed to maintain the cavity at 400 K during cryogenic operation.

The cavity core is instrumented with two platinum variable resistance temperature sensors symmetrically embedded in the heater section near the apex of the cavity. The source temperature is controlled using a Lakeshore feedback-type controller. The Lakeshore controller can maintain cavity temperature to less than  $\pm 0.1$  K. One of the cavity temperature sensors is used as a monitor for the temperature control electronics.

The calibration source is equipped with a 16-position aperture wheel illustrated in Fig. 5. The aperture wheel contains 15 apertures and one blank position. The aperture diameters used in the source are listed in Table 3. This selection of apertures provides an output dynamic range of nominally 400 at a constant source temperature. All of the apertures are 0.001-in.-thick electro-formed nickel pinholes, mounted in counter-bored holes. Position of the aperture wheel is controlled by a bidirectional stepping motor. A rotary potentiometer, connected through a rotary coupling to the rear motor shaft, monitors the wheel angular position. An emitter diode/photo-transistor pair viewing through a slit in the aperture wheel also provides an indication of the aperture wheel position. A cooling strap, connected between the aperture-wheel hub and the source housing, aids in aperture-wheel cooling.

A two-bladed, rotating disc chopper is used to modulate the continuous output from the source. The chopper blade is driven with a variable-speed motor and provides a variable chopping frequency between 10 and 100 Hz. The side of the chopper blade that faces the source is polished to reduce the surface absorption/emissivity. The outer surface is black anodized. A chopped signal at the chopper frequency is provided as a reference signal for AC detector signal measurements. This reference signal is generated using one of two photo-transistor, IR emitter pairs. Both pairs are used to indicate when the chopper blade is blocking the source output aperture, or when it is in the open position. Note that the chopper is removed from the SIRS III assembly when the source is calibrated at NIST or in the UHV chamber.

## **2.4 FOCAL PLANE CHARACTERIZATION CHAMBER SOURCE**

The Focal Plane Characterization Chamber (FPCC), described in Ref. 1, is an AEDC test facility which provides a radiometric characterization of focal plane arrays. The source package is located inside the chamber liner and provides both flood and spot source test capability. Figure 6 is a photograph of the source package as installed in the FPCC. The source mount is cooled to a temperature of less than 20 K. The blackbody source in the FPCC is a design similar to the blackbodies described above. The FPCC source package includes the blackbody cavity emitter, aperture wheel, and chopper assembly. The FPCC source package also includes an optical diffuser wheel, a spectral filter wheel, and an internal translation stage.

The blackbody source is a re-entrant conical cavity which is typically operated at 200 to 500 K. The aperture wheel contains six apertures and one blank position to provide a dynamic range of approximately 400. The aperture diameters are listed in Table 4. The aperture wheel is driven by a stepping motor with a rotary potentiometer to measure position. The chopper is a two-blade, rotating element located in front of the source to modulate the output. The chopper operating frequencies can be varied from 10 to 100 Hz in the two-blade configuration.

The blackbody and the aperture wheel are mounted on a linear translation table to allow the cavity to be driven toward or away from the diffuser. This provides additional control of the FPA irradiance. The spectral filter wheel contains eight filters and one open hole position to spectrally filter the source. Position of the spectral filter wheel is controlled and monitored similar to the aperture wheel.

## **2.5 TRANSPORTABLE DIRECT WRITE SCENE GENERATION SOURCE**

The blackbody source assembly for the Transportable Direct Write Scene Generator (TDWSG) Radiometric Calibration Monitoring System (RCMS) Blackbody Chamber contains a re-entrant conical cavity radiator with an aperture wheel, filter wheel, and chopper wheel (Fig. 7). The blackbody source is a multiple aperture version of the standard infrared source (SIRS) configuration designed and fabricated at AEDC. The source was designed to operate up to a maximum temperature of 800 K and uses apertures ranging in diameter up to a

maximum of 0.100 in. The cavity material for the blackbody core is stainless steel. The parts that compose the interior of the cavity were roughened by air-jet abrasion and then chemically cleaned with solvents and acid-etched. The entire emitter assembly was blackened by oxidation in atmosphere at a temperature of approximately 1150 K. The oxidized surface provided an emissivity greater than 0.85. The effective cavity emissivity is greater than 0.99. A thin wire is wound around the cavity to heat it to the desired operating temperature (from 300 to 800 K). Cavity temperature is measured using two platinum resistance temperature devices (RTDs) potted deep into the blackbody emitter adjacent to the conical cavity. The calibration is accomplished using the resistance of the platinum sensors.

Output apertures are mounted on a wheel that is directly coupled to a stepper motor. This wheel contains six apertures and a blank (no output) position. The blank position provides a zero output condition for evaluation and correction of background effects. The aperture diameters are listed in Table 5. The aperture wheel is positioned with a direct-coupled stepper motor. Cooling of the aperture wheel is accomplished by the use of a copper braid cooling strap attached to the wheel and to the 20 K housing.

A filter wheel is provided in the assembly for use in selecting the desired spectral bandpass. The wheel contains eight filter positions with mounting provision for 1-in.-diam filters. Some of the positions are blanked off and used to evaluate radiometric background within the dewar. The wheel is driven by a direct-coupled stepper motor.

A mechanical chopper is located between the blackbody aperture and the filter wheel. This chopper provides modulation of the blackbody for calibration of detectors and focal plane array diagnostics. It also provides an additional shutter mechanism for background diagnostics. The chopper consists of a symmetrical two-blade wheel. Chopper speed can be controlled over the frequency range of nominally 10 to 100 Hz.

Instrumentation for monitor and control of the source unit includes an aperture wheel control, filter wheel control, chopper control, IR source monitor, temperature controller, and system voltmeter. The RTDs used in the emitter of the blackbody are platinum wire-wound elements that were calibrated by the AEDC Precision Measurement Equipment Laboratory (PMEL).

## **2.6 VARIABLE APERTURE BLACKBODY SOURCE**

The variable aperture blackbody source (VABS) assembly (Fig. 8) is the same source package that was originally designated as the extended source package when it was used in the early 1980's for the Miniature Vehicle (MV) tests at AEDC. The radiation source is a conical blackbody cavity, with a 1.125-in. opening and a 28-deg cone angle. The interior of the cavity is anodized to achieve a surface emissivity greater than 0.95. The effective emissivity of the cavity was calculated to be greater than 0.99 (Gouffe method). The cavity source is heated with a platinum wire wound around the cavity core. The cavity core is

instrumented with three temperature sensors (platinum resistance thermometers) imbedded deep inside the cavity block. Maximum operating temperature of the cavity source is 400 K. A stainless-steel radiation shield provides thermal isolation between the source and its low-temperature mount. All internal surfaces of the shield are polished to reflect the radiated energy to reduce heat loss.

The VABS source assembly includes an aperture wheel that contains eight apertures and a blank position (Table 6). The apertures vary in diameter from 0.0298 in. to nominally 1.0 in. Each aperture has a field stop between it and the cavity core. The field-stop apertures are mounted in a second wheel that is mechanically attached to the wheel containing the output apertures. A cooling strap, attached between the wheels, provides conductive cooling to the wheel assembly. A temperature sensor (silicon diode) is mounted on the wheel assembly to measure the wheel temperature. The aperture/field-stop wheel is driven with a bidirectional stepping motor (0.72 deg/step, 50 steps between aperture positions). A rotary potentiometer is used to monitor the wheel angular position.

## **2.7 SHORT WAVELENGTH INFRARED SOURCE**

The short wavelength infrared (SWIR) blackbody source was developed at AEDC to specifications which make it compatible with the cryogenic/vacuum environment of a space chamber. A maximum operating temperature of 1200 K provides a significant increase in temperature and radiant exitance capability from the previous 500 K low-background blackbody design.

The SWIR source design is illustrated in Fig. 9. The heater core of the blackbody has a conical shape and is made of 304 stainless steel. The interior of the core cavity was roughened by air-jet abrasion and blackened to provide a surface emissivity greater than 0.85. The effective cavity emissivity is greater than 0.98. The core is heated with 0.0126-in.-diam Nichrome® wire and has two imbedded thermocouples to monitor core temperature. One is located near the apex of the inner cone, and the other is located within one of the heater insulators alongside the core. A 0.125-in.-diam alumina insulator provides the core support and thermally isolates the core from the base. A 15-deg maximum field of view (FOV) is provided with this source using a 0.070-in.-diam output aperture. The output orifice for the blackbody is mounted in a copper disk that was attached to the housing by screws using an indium gasket for improved thermal conductance. The output aperture used in calibration was a bimetal electro-formed disk containing a 0.010-in.-diam aperture. The small aperture size was selected to minimize the source output radiation during calibration transfer.

### 3.0 NIST CALIBRATION RESULTS

The source calibrations are performed at the NIST LBIR calibration facility in Gaithersburg, MD. The LBIR facility is described in Ref. 2. The facility includes a vacuum chamber capable of operating below  $10^{-9}$  torr with an optically tight gaseous helium-cooled liner that is cooled to less than 20 K. An absolute cryogenic radiometer (ACR) is used to measure the blackbody output.

Integration of the blackbody into the LBIR facility requires mounting of the blackbody on a standard gold-plated copper plate as shown in Fig. 10. AEDC modified the plate to raise the blackbody aperture to the centerline of the ACR and provided a blackened shroud around the blackbody assembly to minimize stray background, so that the ACR would only see the energy from the blackbody aperture. A reference surface (Invar<sup>®</sup> tab) was provided on the front corner of the plate to provide an accurate measurement of the distance from the blackbody aperture to the ACR.

The calibration procedure at NIST is to measure the total radiant flux from the blackbody with the ACR. Data are recorded for each aperture position at the specified temperature settings. Prior to each measurement, the background flux is recorded with the aperture wheel in the blank position (no blackbody output). The background is then subtracted from the measured flux to determine the radiant flux emitted solely by the blackbody. ACR data at each condition are determined by reading the electrical parameters every second for a 3-min period. The average value and standard deviation of the radiant power are then stored. Each data point of radiant power is also converted to blackbody radiant temperature (Ref. 3) and compared to the readings of the two temperature sensors in the blackbody. Final temperature results are provided as a polynomial equation for each aperture which shows the relationship between radiance temperature and blackbody temperature for each of the two sensors. Three sets of data were taken at each blackbody condition to determine repeatability of the measurements.

NIST estimates diffraction losses for each aperture in the beam path using the procedures published in Refs. 4 and 5. Accounting for diffraction losses required increasing the radiant flux measured at the ACR, and therefore, the radiance temperature of the source. The methods used to calculate the diffraction correction have an estimated systematic error of  $\pm 20$  percent. The NIST-applied diffraction correction has been questioned at AEDC because linearity data taken during calibration transfers have shown the correction to be too high (Ref. 6).

### **3.1 SIRS IIA CALIBRATION**

#### **3.1.1 FY90 Calibration**

A detailed description of the NIST calibration process and the results of the FY90 calibration are described in Ref. 3. The calibration of the SIRS IIA was performed in February 1990 and was the first for AEDC in the LBIR facility and the second source calibration for the new facility. The final report was received from NIST in February 1991 and is referenced as NIST Test No. 534/LBIR-2-90. NIST calibration reports are not available through the Defense Technical Information Center (DTIC).

Table 7 provides the calibration equation and coefficient values for radiant temperature versus blackbody temperature for each aperture and temperature sensor. NIST reports the estimated uncertainty in predicting the radiance temperature using these equations to be  $\pm 0.1$  to  $\pm 0.7$  percent. Table 8 presents a summary of NIST calibration results for SIRS IIA temperature Sensor A and Aperture 3 in terms of temperature, radiance, and radiance uncertainty. The diffraction correction percentages used to increase the measured radiant flux are provided in Table 9. This calibration reestablished AEDC traceability to NIST in low-background and low-temperature blackbody flux.

#### **3.1.2 FY93 Calibration**

In September 1992, the SIRS IIA was again sent to NIST for calibration. Several issues were involved in sending SIRS IIA back to NIST. One was to establish calibration repeatability on the source. NIST had also made several changes to the LBIR facility since the first SIRS IIA calibration. Another issue was that the NIST calibration results for the SIRS III (next section) and transfer calibrations between SIRS III and SIRS IIA at AEDC indicated a substantial discrepancy in results. It was hoped that a return of SIRS IIA to NIST would answer the questions these data raised.

The second NIST calibration of SIRS IIA was completed in early FY93, and the report (844/LBIR-6-93) was received in April 1993. Table 10 provides the calibration equation and coefficient values for radiant temperature versus blackbody temperature for each aperture and temperature sensor. NIST reports the estimated uncertainty in predicting the radiance temperature using these equations to be  $\pm 0.1$  to  $\pm 1.3$  percent. Table 11 presents a summary of NIST calibration results for SIRS IIA Temperature Sensor A and Aperture 3 in terms of temperature, radiance, and radiance uncertainty. The diffraction correction percentages used to increase the measured radiant flux and radiant temperature are provided in Table 9.

### 3.1.3 FY90 and FY93 Calibration Comparison

A comparison of the FY90 and FY93 calibration results for SIRS IIA is provided in Tables 12 and 13. Table 12 compares the FY90 and FY93 NIST calibration equation coefficients for temperature Sensor A for all six apertures. Table 13 summarizes the comparison of radiometric and measured temperature difference, and measured and radiometric radiance difference at five different operating temperatures for Aperture 3. The FY93 NIST calibration results indicate a higher difference between the NIST radiance temperature than that measured by the blackbody sensors (relative to the FY90 NIST calibration). It is interesting, however, that the calibration equation coefficients (Table 12) for FY93 are more nearly linear ( $A_1$  closer to one), with less offset ( $A_0$  closer to zero).

### 3.2 SIRS III CALIBRATION (FY92)

The SIRS III blackbody source was calibrated at NIST in March 1992. Results were provided to AEDC in report, NIST Test No.: 844/LBIR-4-92 dated August 24, 1992. In April 1993, NIST forwarded corrections to apply to the radiant power and radiance temperature results, respectively. The data referenced in this report include those latest correction factors.

Table 14 provides the calibration equation and coefficient values for radiant temperature versus blackbody temperature for each aperture and temperature sensor. NIST reports the estimated uncertainty in predicting the radiance temperature using the corrected equations to be  $\pm 0.1$  to  $\pm 1.3$  percent. Table 15 presents a summary of NIST calibration results for SIRS III temperature Sensor A and Aperture 16 in terms of temperature, radiance, and radiance uncertainty. The diffraction correction percentages used to increase the measured radiant flux and radiant temperature are provided in Table 16.

## 4.0 AEDC CALIBRATION TRANSFER TECHNIQUE

A null calibration technique has been used for many years to calibrate sources at AEDC (Ref. 7). The calibration technique is based on the idea that the test source and the standard source both provide the same approximate output energy, at the same operating temperature. This produces the same input energy to the detector, thus the detector behaves as a null-type detection device. Detector linearity was therefore not critical to the calibration process. However, calibration of a high-temperature (1200 K) source provides a much higher thermal output than does the reference standard and requires a modified calibration transfer technique.

The apparatus used to perform source calibrations is illustrated in Fig. 11. This figure illustrates the orientation of the test hardware within the envelope of the UHV Chamber. The major hardware components within the chamber are the two blackbody source assemblies

and either the bolometer or the Si:Ga detector. The bolometer installation is shown in Fig. 11. Support hardware for these components include the source translator and the data acquisition and control hardware.

#### **4.1 ULTRA-HIGH VACUUM TEST CHAMBER**

The UHV Research Chamber is used to perform the radiometric calibration of blackbody sources. Vacuum pumping to nominally  $10^{-5}$  torr is provided by a turbo-molecular pump, backed by a mechanical vacuum pump. The chamber has a light-tight liner which is GHe-cooled to provide a 20 K environment. The liner provides additional cryopumping which lowers the chamber pressure to nominally  $10^{-7}$  torr. The liner contains four bulkhead connectors. Cables from the four connectors within the chamber wrap around the liner to prevent heat from conducting into the chamber hardware. The other ends of the cables are connected by way of vacuum feedthroughs at the UHV chamber shell wall to instrument racks in the laboratory. This cabling system allows internal hardware or the liner to be removed from the chamber vacuum shell as independent units with only minor disconnects required.

##### **4.1.1 Source Platform Assembly**

The source platform assembly serves as the interface for either two or three blackbody sources, the chopper assembly, and a filter wheel (Fig. 11). The assembly consists of a fixed baseplate and a front plate. These plates are actively cooled to 20 K with GHe to provide conductive cooling to the attached hardware. The baseplate is mounted to the floor plate inside the UHV Chamber liner. The front plate of the assembly (Fig. 11), which faces the bolometer, is connected to the baseplate. The chopper motor and filter wheel motor housings extend toward the bolometer. Between the two motors is a single opening which is aligned to the bolometer element.

The chopper wheel is installed directly on the front plate of the platform assembly. The chopper wheel (two-blade configuration) is required to modulate the source radiation output. Blade heating is minimized by conductively cooling the motor mount through the front plate. The side of the chopper blade that faces the source is polished to reduce the surface emissivity. The outer surface is black anodized. A reference signal from the chopper is needed for an input to the phase-lock amplifier. This reference signal is generated using a photo-transistor IR emitter pair, mounted 180 deg from the source opening. The signal from the photo-transistor IR emitter pair also provides absolute indication as to when the chopper blade covers, or uncovers, the source output aperture.

The filter wheel is mounted between the source aperture(s) and the chopper wheel. As described above, the stepping motor for the filter wheel is mounted to the front plate of

the platform. The filter wheel was used only in the open hole and blanked positions for the calibrations presented in this report. The blanked position provided a tare readout of the detector output. This tare was compared to the tare reading obtained with the test source blanked by its aperture wheel.

For source calibrations, two sources are installed on a translating drive platform in the UHV. The translation drive provides the mechanism to align each source aperture with the bolometer through the exit hole in the front plate. A ball screw translation design is incorporated into the source platform assembly. Beneath the platform are the drive screw nut assembly and three linear bearings. Two of the linear bearings are aligned along one edge of the plate, and the other is centered at the edge of the opposite side. These items are attached to the drive screw assembly and linear bearing rails, which in turn are mounted to the baseplate of the source platform assembly. The ball nut is preloaded by the manufacturer to prevent backlash when the translator is stopped at a desired position. The ball screw is driven by a stepping motor, which is coupled to the screw through a sprocket and chain drive assembly. The motor is coupled to a potentiometer through a flexible coupling to the rear shaft of the motor. The potentiometer turns three complete revolutions for each rotation of the screw. An optical encoder disc on the end of the drive screw provides a pulse for each revolution of the drive screw. Two microswitches, one for each direction, are used to stop the motor drive at the limit of the platform travel.

#### **4.1.2 Data Acquisition and Control System**

The data acquisition and control system for three source assemblies installed in the UHV Chamber is illustrated in Fig. 12. A constant current source provides the bias current for the temperature sensors. Sensor resistance is calculated from measured current and voltage outputs. The current is determined from a voltage drop measurement across a precision resistor. The voltage output from the temperature sensing resistors is measured using a precision digital voltmeter. A Lakeshore Cryotronics temperature controller is used to maintain cavity temperature to within  $\pm 0.01$  K. One of the cavity temperature sensors was used as a monitor for the temperature control electronics.

The translation platform motor drive controller is a UNIDEX 11, with an AEDC-designed and fabricated current limiter and a DC power supply (0-20 volts). The potentiometer position readout for the translator was also designed and fabricated at AEDC. The potentiometer bias, zero, and span adjustment are provided in the chassis with the digital position readout. The AEDC-designed and fabricated optical encoders monitor the position of a slotted wheel on the linear translator and on the SIRS source aperture wheel. The SIRS aperture wheel drive and position readout are also of AEDC design.

An Apple II+ computer is used to monitor applicable test parameters. The computer converts voltage/current sensor outputs to engineering units (Kelvin). Data are manually recorded from the computer video monitor.

## **4.2 IR LABS BOLOMETER TECHNIQUE**

### **4.2.1 Bolometer System**

A bolometer is a broadband thermal detector that has a large change in resistance in response to heating from incident radiation. The germanium bolometer element used for source calibration was suspended in a small gold-coated cavity within its mount. The gold cavity produces multiple reflections of the incoming radiation, which provides for uniform radiant heating of the bolometer element. The bolometer is coated on both sides with 3M® Nextel Black Velvet paint. This paint provides the broadband absorption characteristic of the bolometer. The front of the bolometer mount cavity contains cold field stops and apertures to limit the FOV of the element to minimize the extraneous input of chamber stray background radiation.

The bolometer dewar is needed to cool the bolometer to its operating temperature of nominally 2 K. An overall schematic of the LHe dewar system is shown in Fig. 13. The bolometer dewar is basically a stainless-steel cylinder, 15.2 cm in diameter by 15.2 cm deep. The bottom of the cylinder is a brass disc 0.95 cm thick. The bolometer is mounted to a copper bracket, that mounts directly to the brass disc. The dewar holds 2.7 liters of liquid and has a hold time of approximately 8 hr.

The bolometer dewar is filled from a 500-liter LHe storage dewar. The liquid transfer line from the 500-liter dewar connects to the bolometer transfer line at a Linde bayonet quick disconnect fitting. The transfer line from the storage dewar has a single vacuum-jacketed supply tube. The bolometer dewar transfer line is of a tri-axial design with the LHe flow in the inner tube, the dewar return vent in the center tube, and an outer vacuum jacket. After the bolometer dewar is filled from the storage dewar, the transfer line is disconnected at the bayonet. A rubber stopper is inserted in the LHe inner tube of the bolometer transfer line, the vent valve is closed, and the bolometer dewar is evacuated using a Welch Duo Seal Model 1402 vacuum pump. Dewar pressure is monitored using an MKS Baratron 1,000-torr transducer. The pressure is monitored using an MKS PDR-C-2C power supply and readout. The LHe temperature is determined from the bolometer dewar pressure. Bolometer responsivity is a function of the LHe dewar pressure (i.e., temperature). However, the bolometer responsivity/He dewar pressure relationship does not repeat between dewar fills (Fig. 14). Therefore, the bolometer responsivity is measured using a standard blackbody source.

The data acquisition system for the bolometer is shown in Fig. 15. The signal conditioning unit provides the bolometer bias and impedance matching, and includes heater control for the Junction Field Effects Transistor (JFET). The bolometer signal output is measured using a phase-lock amplifier. A reference signal from the radiation source chopper reference element is input to the phase-lock amplifier. Dewar pressure is measured using an MKS Baratron pressure measurement system.

#### 4.2.2 Test Description

The first step of calibration in the UHV Chamber is to evacuate the chamber and cool the internal test hardware (with exception of the source cavities) to nominally 20 K. The next step is to fill the LHe dewar to cool the bolometer. A vacuum pump connected to the LHe dewar evacuates the helium system to nominally 20 torr, thus reducing the LHe temperature to nominally 2 K. The cavity temperature of the sources is set to 200 K.

Calibration of a low-temperature source (500 K maximum) begins with positioning the SIRS IIA source to irradiate the bolometer. A source aperture is selected to provide a bolometer signal above 100 mv. The phase between the chopper reference and the bolometer signal is adjusted to maximize bolometer signal output. The aperture wheel is driven to the smallest aperture position. The bolometer signal, source temperature, source aperture, and all housekeeping parameters are recorded. The test source is then positioned to illuminate the bolometer. The same procedure, described above for the SIRS, is followed to record the bolometer signal for each of the test source apertures until the bolometer instrumentation signal saturation is reached. The two sets of data thus recorded provide the information needed to calculate the bolometer sensitivity and the measured test source radiometric output. The cavity temperature of the two sources is then raised to the next increment (50 K), and the procedure repeated. Calibration data are recorded in 50 K increments from 200 to 400 K (temperature limit of SIRS IIA).

Detector linearity is not an issue when performing the null calibration transfer between two sources of similar temperature and radiometric output. However, high-temperature source calibration (600 to 1200 K) requires use of three sources and a slight modification of the test technique. The SWIR source, for example, is calibrated using the output from the bolometer detector, which is not a null measurement. The absolute calibration of the bolometer is dependent on the bolometer element temperature. Since it is not possible to maintain the bolometer at a constant temperature throughout the calibration test period, it is calibrated prior to the SWIR source measurements. The bolometer linearity is also essential to the SWIR source calibration because the output radiation from the SWIR source is much larger than that from the SIRS IIA source. A small (0.010-in.-diam) output aperture is used on the SWIR source to provide a better radiometric output match to the bolometer. Bolometer linearity

is established using the SIRS IIB source, using the selectable aperture opening sizes. The linearity of the source output with aperture area is a major assumption of the SWIR source calibration. A set of linearity data is also taken at each SWIR source calibration run.

#### 4.2.3 Calculations

The broadband radiated power collected by the bolometer detector is determined by the hardware geometry and the radiation from the source cavity. The broadband radiant exitance from a blackbody emitter is the product of the Stefan-Boltzmann constant times the fourth power of the source temperature. The irradiance at the bolometer is calculated as follows:

$$E = 0.45(A_s S T^4)/(\pi d^2) \quad (1)$$

where

0.45 = chopper modulation factor

$A_s$  = area of source aperture,  $\text{cm}^2$

$d$  = distance from source aperture to detector aperture, cm

$E$  = source irradiance,  $\text{W cm}^{-2}$

$T$  = source temperature, K

$S$  = Stefan-Boltzmann Constant,  $\text{W cm}^{-2} \text{T}^{-4}$

This equation assumes a point source ( $d$  is at least ten times the source aperture and bolometer diameters) and a unity emissivity for the blackbody.

The bolometer irradiance responsivity is the bolometer output voltage divided by the irradiance at the bolometer:

$$R_E = V/E \quad (2)$$

where

$R_E$  = bolometer responsivity,  $\text{mv/W/cm}^2$

$V$  = bolometer output, mv

The bolometer responsivity is determined using the bolometer output when it is irradiated by the SIRS source. The output from the test source is calculated using the above bolometer responsivity as follows:

$$E = V/R_E \quad (3)$$

A source irradiance comparison is used to transfer the SIRS IIA calibration to high-temperature (> 400 K) test sources.

The bolometer flux responsivity is used to transfer the calibration between low temperature sources ( $\leq 400$  K). The flux collected by the bolometer is the product of the irradiance times the bolometer collection area.

$$\Phi = EA_d \quad (4)$$

where

$$A_d = \text{bolometer area, cm}^2$$

The flux responsivity is the bolometer output voltage divided by the flux.

$$R_\Phi = V/\Phi \quad (5)$$

where

$$R_\Phi = \text{bolometer responsivity, mv/W}$$

$$\Phi = \text{flux incident on bolometer, W}$$

### 4.3 Si:Ga DETECTOR TECHNIQUE

The UHV Chamber installation with the Si:Ga detector is similar to that using the bolometer. In this case, the detector is inside a dewar which is mounted on the end flange of the chamber. The distance from the source to the detector is larger in the Si:Ga detector configuration than the bolometer configuration.

#### 4.3.1 Detector System

The detector system includes a Si:Ga detector, a LakeShore dewar, and detector signal conditioning electronics. The Si:Ga detector is 1-mm square and has a transparent contact on its irradiated surface. It is a low-background device with a long wavelength cutoff at nominally 18  $\mu\text{m}$ . The detector peak normalized spectral response is presented in Fig. 16. The detector peak responsivity is nominally 1.2 A/W (12 volt bias, 15 K, 12.8  $\mu\text{m}$ , and 25 Hz). The detector is a bulk type and exhibits nonlinear response at low background as a result of dielectric relaxation effects (DRE). The response nonlinearity is depicted in the lower set of data presented in Fig. 17. The detector's region of linearity is very good if the detector is operated at a slightly elevated radiometric background (upper set of data in Fig. 17). The

detector is usually operated at a temperature of 15 K, with the radiation input chopped at 25 Hz and with a nominal  $10^{12}$  photon/cm<sup>2</sup>/sec background flux.

The detector is mounted in a LakeShore Model MTD150 (Modular Test Dewar). Liquid helium is supplied to the dewar from a 500-liter liquid helium storage dewar. The flexible transfer line is vacuum-insulated with a bayonet connection to the MTD150, and a long rigid withdrawal tube that is inserted in the 500-liter storage dewar. A flow valve controls the flow of cryogen through the transfer line. An electrical heater attached to the detector mount maintains the detector temperature at a desired set point. Heater power is supplied and then temperature-controlled using a LakeShore temperature controller. The controller provides detector temperature stability of  $\pm 0.01$  K. Cool-down and warm-up times are typically 50 and 20 min, respectively. Detector electrical connections are provided at the MTD150 baseplate.

The detector output is measured through a trans-impedance amplifier (TIA) that has three individually selected feedback resistors. The feedback resistors have nominal resistance values of  $10^7$ ,  $10^8$ , and  $10^9$   $\Omega$ . The TIA electronics are mounted on the MTD dewar baseplate, close to the detector. The control electronics provide bias adjustment between 0 and 12 volts. The output signal from the TIA is measured using a Stanford Research System phase-lock amplifier. The reference signal to the phase-lock amplifier is provided for the UHV chopper electronics.

#### **4.3.2 Test Description**

The first step for source calibration in the UHV Chamber is to evacuate the chamber and cool the internal test hardware (with exception of the source cavities) to nominally 20 K. The next step is to fill the LakeShore dewar with LHe to cool the Si:Ga to its operating temperature of 15 K. The cavity temperatures of the sources are then set to 200 K.

The SIRS IIA source is positioned to irradiate the detector. The aperture wheel is driven to the smallest aperture position. The detector signal, source temperature, source aperture, and all housekeeping parameters are recorded. The same procedure, described above for the bolometer, is followed to record the detector signal for the test source apertures. The cavity temperatures of the two sources are then raised to the next increment (50 K or 100 K), and the procedure repeated. Calibration data are recorded in increments from 200 to 500 K. Note that the SIRS IIA is limited to 400 K.

#### **4.3.3 Calculations**

The radiated power collected by the Si:Ga detector is determined by the hardware geometry, the radiation from the source cavity, and the normalized spectral response of the detector. The power received by the detector is calculated as follows:

$$P = \frac{0.45 A_d A_s}{d^2 \pi} \int_{\lambda_1}^{\lambda_2} \frac{c_1 R_n(\lambda)}{\lambda^5 (e^{(c_2/\lambda T)} - 1)} d\lambda \quad (6)$$

where

0.45 = chopper modulation factor

$A_s$  = area of source aperture,  $\text{cm}^2$

$A_d$  = area of Detector,  $\text{cm}^2$

$c_1$  =  $3.7415\text{E}04 \text{ W}\mu\text{m}^4/\text{cm}^2$

$c_2$  =  $1.43879\text{E}04 \mu\text{m K}$

$R_n(\lambda)$  = normalized spectral response of the Si:Ga detector

$\lambda$  = wavelength,  $\mu\text{m}$

$d$  = distance from source aperture to detector aperture, cm

$P$  = power received by detector, W

$T$  = source temperature, K

Equation (6) assumes a point source ( $d$  is at least ten times the detector and source aperture diameter) and a unity emissivity for a blackbody. The area of the Si:Ga detector is  $0.01 \text{ cm}^2$ . The distance between the source and detector is typically 22.9 in. for the SIRS IIA and B. The distance for the other sources varies depending on the installation. A BASIC program is used to calculate the integral. Integration over the wavelength range of 1 to 21 micrometers is normally used, since that is the spectral range of the Si:Ga detector.

The detector responsivity is defined as the detector output current divided by the incident radiant power (Eq. (3)):

$$R = I/P \quad (7)$$

where

$R$  = Si:Ga detector responsivity, A/W

$I$  = detector output current, A

$P$  = power on the detector, W

The detector output current is calculated from the measure output voltage as follows:

$$I = V/(1000R_{fb}) \quad (8)$$

where

$V$  = detector output voltage, mV

$R_{fb}$  = feedback resistance,  $\Omega$

The value of the feedback resistor is dependent on the gain setting. The medium gain has a  $9.2E07 \Omega$  resistor. The high gain is a  $9.8E08 \Omega$  resistor.

## 5.0 AEDC CALIBRATION TRANSFER RESULTS

The transfer of the SIRS IIA calibration (calibrated at NIST) to other blackbody sources at AEDC is accomplished in the AEDC UHV chamber. The SIRS IIA blackbody source calibration is transferred to other sources through either a bolometer or Si:Ga detector. For low-temperature ( $\leq 500$  K) sources, the bolometer or detector responsivity is used as the comparison parameter for the performance of the test source relative to the standard source. The cavities for both the test and standard sources have to be at the same temperature when using the Si:Ga detector because the relative spectral response of the Si:Ga detector is not accurately known. The percent deviation of the detector responsivity is a measure of the performance of the test source, with zero-percent deviation inferring that the radiance of the test source is identical to the standard source. The transfer of the NIST calibration to high-temperature sources is obtained using the AEDC bolometer. The standard of performance for high-temperature sources is the comparison of the irradiance at the bolometer based on the source cavity temperature and output aperture area, and the irradiance measured by the bolometer. The bolometer irradiance responsivity is determined using the SIRS IIA source. As above, a zero-percent deviation between the measured and calculated irradiance corresponds to good test source performance. This method of comparison requires good linearity of the transfer device. Sources calibrated over the past several years also include the SIRS IIB, SIRS III, the TDWSG source, VABS, and the SWIR source. Calibrations of each of the above sources are presented below.

### 5.1 SIRS IIB CALIBRATION

The most recent transfer calibration from the SIRS IIA to the SIRS IIB was performed on April 29, 1992. The test was conducted in the UHV Chamber using the Si:Ga detector operating at 14.9 K and 12 V bias. A performance comparison between SIRS IIA and

SIRS IIB is presented in Table 17. Data were recorded for SIRS IIA and SIRS IIB cavity temperatures of 200, 300, and 400 K. The SIRS IIB source was also run at a cavity temperature of 500 K. The detector responsivity presented for SIRS IIA and SIRS IIB was calculated from the average recorded for all six aperture settings at each source temperature. The low-temperature (200 and 300 K) data were recorded using the high gain setting of the TIA. The medium gain setting was used for the 300, 400, and 500 K measurements. The average percent deviation between the detector responsivity measured, using SIRS IIA and SIRS IIB, was less than 2 percent. The greatest deviation (4.5 percent) was measured at a cavity temperature of 200 K, using the high TIA gain.

## 5.2 SIRS III CALIBRATION

Prior to sending SIRS III to NIST, a transfer calibration of SIRS III blackbody source relative to SIRS IIA was performed in the UHV Chamber. The UHV test was performed in January 1992 using the Si:Ga detector as the transfer device. The test results are shown in Fig. 18. The Si:Ga detector responsivity is plotted as a function of incident power for both blackbody sources. The data presented were for cavity temperatures of 400 K, 12 volt detector bias, 14.8 K detector temperature, medium TIA gain, and a 25-Hz chopping frequency. The decrease in detector responsivity at decreasing incident power levels (Fig. 18) resulted because of the low chamber background flux and the detector DRE problem. The detector responsivity measured, using the two sources, was in very good agreement for power levels above  $1\text{E} - 10$  W. The greatest difference in responsivity was recorded for the lowest power input to the detector. When the data were analyzed, it was hypothesized that the responsivity difference resulted because a higher chamber background was incident on the detector when the SIRS III source was positioned in front of the detector.

SIRS III was sent to NIST for calibration in March 1992. The NIST data indicate that the radiometric output from SIRS III is not linear with source aperture area for the smallest aperture (Fig. 19), and that the source radiometric temperature was significantly different from the indicated cavity temperature recorded by the cavity temperature sensors. (Note that these data were from the original NIST SIRS III calibration report, and that the NIST data were corrected in a letter sent to AEDC in April 1993.) As a result of this anomaly, the SIRS III source was again evaluated in the UHV Chamber (June 1992). The SIRS III radiant output was again compared to that from the SIRS IIA source using the Si:Ga detector. However, the UHV background source was used to alleviate the detector DRE problem. Data were recorded for all source apertures (15 in SIRS III and 6 in SIRS IIA) for cavity temperatures of 200, 300, and 400 K. In addition, SIRS III data were recorded at all aperture positions for a cavity temperature of 500 K. The low-temperature (200 and 300 K) data were recorded using the high gain TIA setting. The medium gain TIA setting was used for the 300, 400, and 500 K measurements. The results of the SIRS III source measurements are presented

in Fig. 20. The legend lists the source temperature and TIA gain ("H" for high gain and "M" for medium gain). With the exception of the 200 K cavity temperature, the detector responsivity is independent of power (e.g., source aperture area). The small aperture, low-temperature data were recorded at very low detector signal-to-noise ratio and are suspect. Note that the detector responsivity increases with increasing cavity temperature. This resulted because the detector-normalized spectral response was not recorded at the same test conditions used during the UHV test. The normalized spectral response for the UHV test conditions is not accurately known.

A performance comparison between SIRS III and SIRS IIA is presented in Table 18. The detector responsivity presented in Table 18 is the average for all aperture settings in each source (15 in SIRS III and 6 in SIRS IIA) at each cavity temperature. The average percent deviation between the detector responsivity measured, using SIRS III and SIRS IIA, was less than 2 percent. The greatest deviation was measured at a cavity temperature of 300 K, using the TIA high gain setting. Note that the percent deviation was only 1.7 percent at that same cavity temperature measurement using TIA medium gain setting. These AEDC data are in good agreement with the corrected NIST data, with the exception of the higher than expected source output from the smallest two apertures.

### 5.3 TDWSG SOURCE CALIBRATION

The transfer calibration of the TDWSG blackbody source relative to SIRS IIA was performed in the UHV Chamber in September 1992. This was the first time this source was tested in the UHV. The main purpose of the test was to determine the operating characteristics of the source (as opposed to an actual calibration). The UHV tests used SIRS IIA as the standard source and the Si:Ga detector operating at 15 K and 12 V bias as the transfer device. The Si:Ga detector was selected instead of the bolometer because the Si:Ga is much easier to operate. The bolometer, however, would be a better choice for a high-temperature source calibration because it has a broader spectral response than the Si:Ga detector. For calibration, the detector is used as a null device when calibrating low temperatures (300 and 400 K), and depends on the detector linearity for the higher source temperatures (500 to 800 K).

A performance comparison between SIRS IIA and TDWSG is presented in Table 19. Data were recorded for the SIRS IIA and TDWSG blackbodies for cavity temperatures of 300 and 400 K. The TDWSG source was also run at cavity temperatures of nominally 500, 600, 700, and 800 K. The 300 K data were recorded using both high and medium TIA gains. The medium TIA gain was used for TDWSG cavity temperatures from 400 to 700 K, and the low TIA gain was used for the 700 and 800 K measurements. The detector responsivity presented for SIRS IIA and TDWSG sources was calculated from the average recorded for all six aperture settings at each source temperature. The percent deviation between the detector responsivity measured, using SIRS IIA and TDWSG, was less than 6 percent for the 300 and 400 K data.

The TDWSG cannot be directly compared to the SIRS IIA source at temperatures above 400 K. However, the change in detector responsivity per 100 K cavity temperature change provides some indication of the TDWSG source performance at the higher temperatures. This performance parameter is labeled as  $\Delta$  in Table 19.

$$\Delta = 100(R_{n-1} - R_n) / R_{n-1} \quad (9)$$

The value of  $\Delta$  (in percent) at 400 K was calculated by subtracting the responsivity at 300 K from the 400 K value, and dividing by the 400 K value. This process was repeated for each subsequent responsivity pair up to a blackbody temperature of 700 K. The percent increase was nominally 4 percent for each temperature increase, indicating good performance for the TDWSG source at the higher cavity temperatures.

#### 5.4 VAB SOURCE CALIBRATION

The transfer calibration of the VABS relative to SIRS IIA was performed in the UHV Chamber in August 1990. The UHV tests used SIRS IIA as the standard source and the AEDC bolometer as the transfer device. The test results of ten data sets are presented in Table 20. The bolometer responsivity was calibrated using the SIRS IIA source (column 2) and compared to the bolometer responsivity calculated using the VAB source (column 3). The 200 and 250 K bolometer responsivity data measured with the VAB source were the average of the data recorded for Apertures 2 through 5 (Aperture position 1 is blank). The 300, 350, and 400 K bolometer responsivity data were the average of the data recorded for Apertures 2 through 4. Data were not recorded for the other larger apertures because of limitations in measuring higher radiometric power inputs to the bolometer.

The average percent deviation between the bolometer responsivity measured, using VABS and SIRS IIA for the ten data sets, was less than 0.8 percent. The greatest deviation (2.7 percent) was measured at a cavity temperature of 250 K. The responsivity deviation was less than 1.2 percent for all of the other data sets recorded.

#### 5.5 SWIR SOURCE CALIBRATION

The transfer calibration of the SWIR blackbody source relative to SIRS IIA was performed in the UHV Chamber in September 1989. The UHV tests used SIRS IIA as the standard source and the AEDC bolometer as the transfer device. This calibration relies on the linearity of the bolometer, as opposed to using the bolometer as a null device when calibrating low-temperature sources.

The bolometer calibration was established using the SIRS IIA standard source. The measured irradiance at the bolometer from the SWIR blackbody source was calculated from the bolometer responsivity. The test results are presented in Table 21 and Fig. 21. The measured irradiance (column 4, Table 21) was compared to that calculated from the SWIR source cavity

temperature, the source aperture area, and the distance from the source to the bolometer (column 3, Table 21). The percent difference between the measured and calculated irradiance is presented in column 5. The effective cavity temperature presented in column 6 was calculated from the measured irradiance. Figure 21 compares the measured and calculated irradiance as a function of cavity temperature.

The measured and calculated irradiance at the bolometer are in very good agreement (> 4 percent) for source temperatures below 800 K. The percentage difference increased to nominally 14 percent as the source temperature increased to 1200 K. The percent difference of the measured data to the calculated data for each given temperature was nominally the same for all of the data. The measured source output (broadband) can be corrected by using an effective source temperature for the SWIR source. This is reported in the last column of Table 21. For instance, the SWIR source output for a measured cavity temperature of 1200 K is actually more nearly that which would be calculated for a cavity source temperature of 1170 K. The cause of this difference in temperatures was probably because of the spectral mismatch between the calibration source at 400 K and the much higher SWIR source temperature, or an error in the SWIR core temperature measurement. A spectral mismatch error would result because of the decrease in spectral absorptance of the bolometer transfer device at short wavelengths. This deviation in effective and measured temperature, however, has little effect on the broadband operation of the source. The spectral radiant exitance of the source as a function of the cavity temperature should be analyzed in the future. Currently, neither NIST nor AEDC has the capability to perform spectral calibrations of blackbodies.

## 6.0 DIFFRACTION CORRECTION MODELING

In 1974, the NBS published Technical Note 594-8 stating that diffraction losses should be accounted for in calculating the radiometric output of IR sources. Since 1979, a diffraction correction has been applied to the radiometric output for all cavity-type blackbody sources in use at AEDC. Following the FY90 calibration of SIRS IIA at NIST, the appropriate application of diffraction corrections to AEDC blackbody sources was reviewed as described in Ref. 6. The theoretically predicted source diffraction losses were examined and compared to experimental data obtained during the calibration of a typical AEDC source. The blackbody linearity results from the experimental data indicate that application of currently available diffraction correction theories is suspect and very likely leads to erroneous results.

As a result of the difference between the experimentally observed SIRS blackbody linearity with aperture area and the results obtained from application of existing diffraction-correction models, the theoretical models or their region of application are very suspect for blackbodies designed and used at AEDC. During FY93 a technology effort was initiated to investigate this problem.

Recent theoretical derivations of blackbody diffraction correction, especially Refs. 4 and 5, are dependent on a number of fundamental assumptions that should be satisfied and verified before application, as should normally be done with any theoretical model. In particular, the current diffraction models, Refs. 4 and 5, are derived from a (Fresnel-Kirchhoff) scalar-diffraction theory. These theoretical derivations are therefore based on source-aperture geometries, diffracting apertures, aperture-detector geometries, and radiation wavelengths such that scalar-diffraction theory applies. These derivations particularly assume that the diffracting aperture is much larger than the wavelength of the radiation being transmitted and subsequently diffracted. The source-to-aperture and aperture-to-detector separation distances are similarly assumed to be much larger than the radiation wavelength being considered for transmission and subsequent diffraction. The more general scalar-diffraction theory of Fresnel-Kirchhoff includes an obliquity factor that more accurately accounts for off-axis source and detector geometries.

The diffraction correction models used in Refs. 4 and 5 also assume on-axis geometries and small source/detector geometries. These small-angle assumptions result in obliquity factors near unity. When the source or detector or both are not small, then the obliquity factors should be included for more accurate diffraction correction calculations. As noted earlier, the AEDC blackbody sources (internal reentrant apertures) are not small in angular extent as viewed from their limiting output apertures, and the application of the diffraction models of Refs. 4 and 5 are therefore expected to be somewhat erroneous. An FY93 technology effort was initiated to examine the current diffraction correction models proposed by NIST for application in blackbody calibration and to develop a more accurate diffraction correction model that includes obliquity factors and the extended Lommel formulation using a Mathematica program. This current effort, the model, diffraction correction calculations, and comparison of the AEDC/NIST blackbody diffraction corrections will be documented in a separate and subsequent technical paper and report.

In addition to diffracted radiation effects, calibration of blackbodies is very much dependent on suppressing extraneous scattered radiation from any surface within the FOV of the detectors. In particular, any additional limiting apertures or surfaces introduced to limit or restrict the emission of radiation from the blackbody cavities act as a source of scattered, stray radiation. This additional extraneous stray radiation may compensate for or far exceed any observable diffraction effects introduced from the normal apertures used in the AEDC blackbodies being used for calibration and sensor testing.

## **7.0 FUTURE CALIBRATION REQUIREMENTS**

Future AEDC calibration requirements are coordinated with NIST through participation in the NIST User's Advisory Board. This group meets approximately every six months to

discuss calibration results and review the NIST LBIR facility capabilities and future plans. These plans currently incorporate AEDC needs in the area of low-background radiometry. NIST expects to have a new spectral facility operational by the end of FY93. A high sensitivity ACR is to be operational for blackbody calibrations beginning in January 1994. The new ACR will provide traceability data for low-temperature and small aperture sources. The low-background IR (LBIR) detector transfer standards (BIB Si:As) will be calibrated both broadband and spectrally in the new LBIR facility. The detectors will not be available until mid-FY94. In late FY94, AEDC will work to acquire a standard detector and spectral calibrations on ND filters and integrating spheres. In FY95 and beyond, AEDC will continue to work with NIST, specifically on obtaining further spectral calibrations, especially on blackbody sources.

Future calibration requirements also involve continuing use of the LBIR blackbody calibration facility. Current plans are to reestablish traceability of the FPCC source (500 K) or a new 800 K source for this chamber. Results of the FPCC blackbody's current calibration were not presented in this report since its traceability is to the SIRS I (Ref. 7) and not to the SIRS IIA. The TDWSG source (800 K) requires either direct NIST calibration or a calibration against the SIRS IIA using the bolometer. The SIRS III blackbody may also be returned to NIST for a repeat calibration in the near future. The development of the Focal Plane Array Test Chamber (IOC in August 1994) may also lead to the calibration of an additional 800 K source.

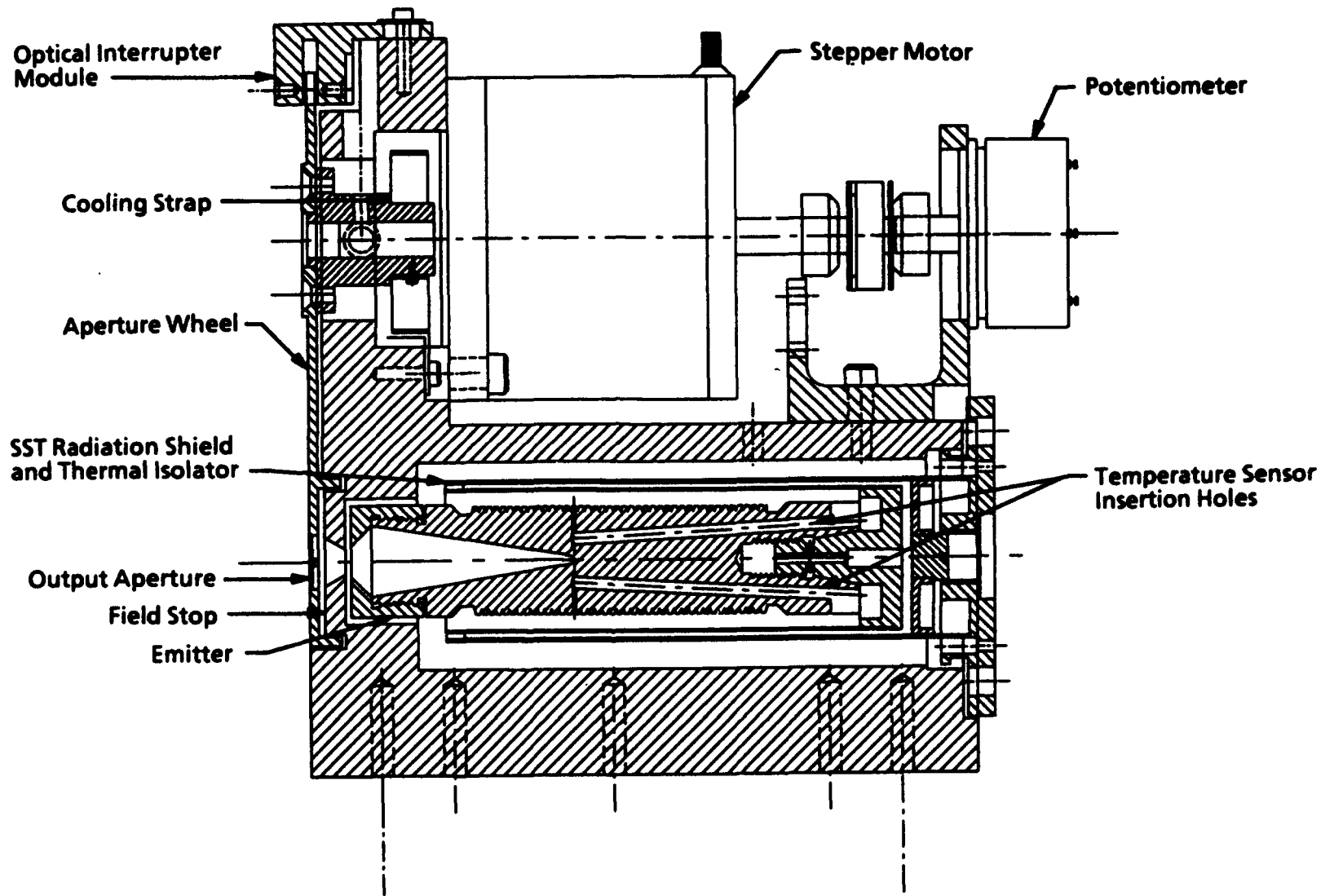
## 8.0 CONCLUDING REMARKS

This report has provided a summary of the status of radiometric traceability of AEDC sources to the NIST. AEDC sources have continually performed well at NIST with calibration corrections of less than 5 percent. The calibration transfer process in the UHV chamber has also proved to be highly accurate as demonstrated by the SIRS III results from direct NIST calibration and transfer from SIRS IIA. Because data are AEDC's primary product, maintaining this traceability to yield low data uncertainties will continue to be a priority in the future.

## REFERENCES

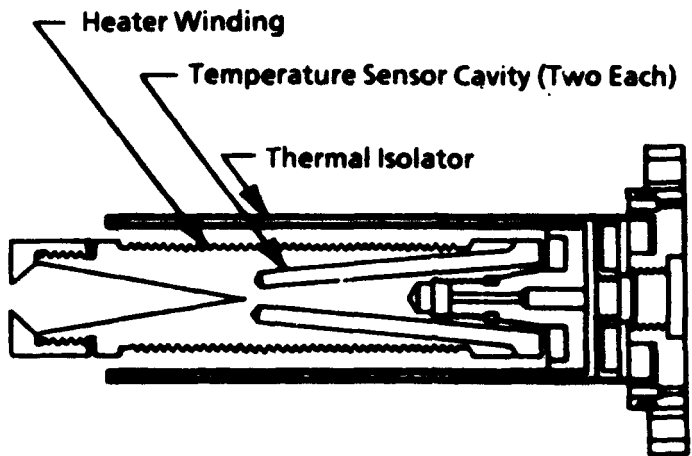
1. Nicholson, R. A. and Steele, C. L. "AEDC Focal Plane Array Test Capability." AEDC-TR-90-31 (AD-A230846), January 1991.
2. Ebner, S. C. and Parr, A. C. "Update on the Low-Background IR Calibration Facility at the National Institute of Standards and Technology." SPIE Vol. 1110 (1989).

3. Jarratt, K. B. "Calibration of an AEDC Low-Temperature Blackbody Standard at NIST." AEDC-TR-91-9 (AD-A245071), January 1992.
4. Steel, W. H., De, M., and Bell, J. A. "Diffraction Corrections in Radiometry." *Journal of the Optical Society of America*, Vol. 62, September 1972, p. 1099.
5. Boivin, L. P. "Diffraction Corrections in the Radiometry of Extended Sources." *Applied Optics*, Vol. 15, May 1976, p. 1204.
6. Young, R. P. and Herron, C. B. "Application of Diffraction Corrections to Blackbody Sources." AEDC-TR-91-4 (AD-A237840), June 1991.
7. Sherrell, F. G. "Infrared Standards to Improve Chamber 7V Beam Irradiance Calibrations." AEDC-TR-80-45 (AD-A094658), January 1981.

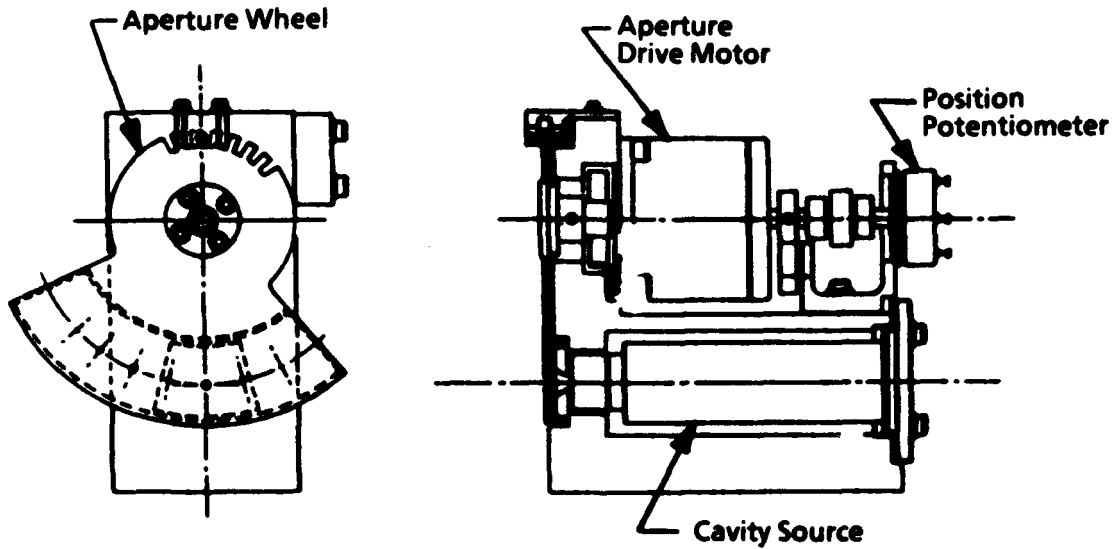


33

Figure 1. Cross-sectional view of SIRS IIA assembly.



a. Cavity source



b. Assembly

Figure 2. SIRS IIB blackbody source.

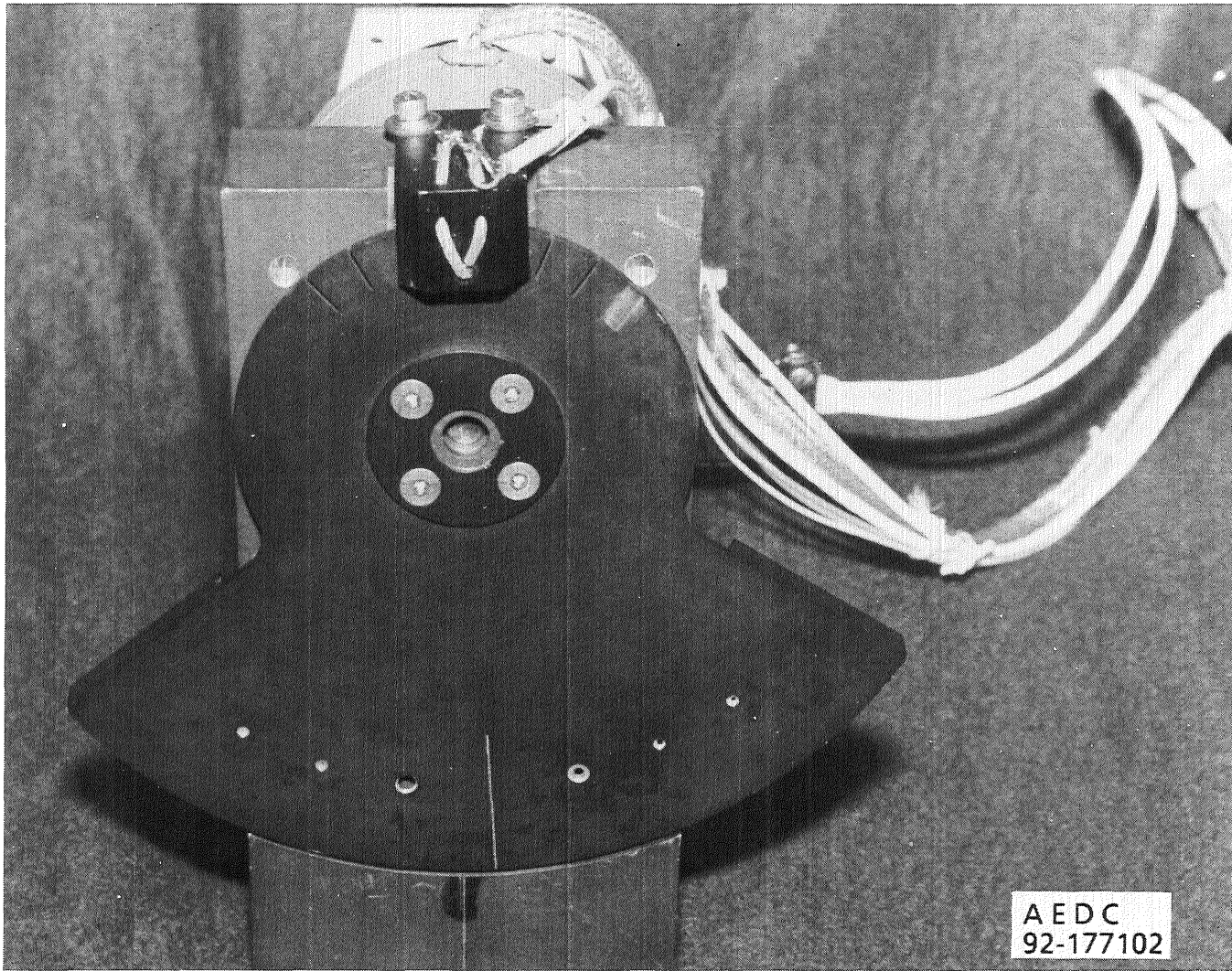


Figure 3. SIRS IIB assembly.

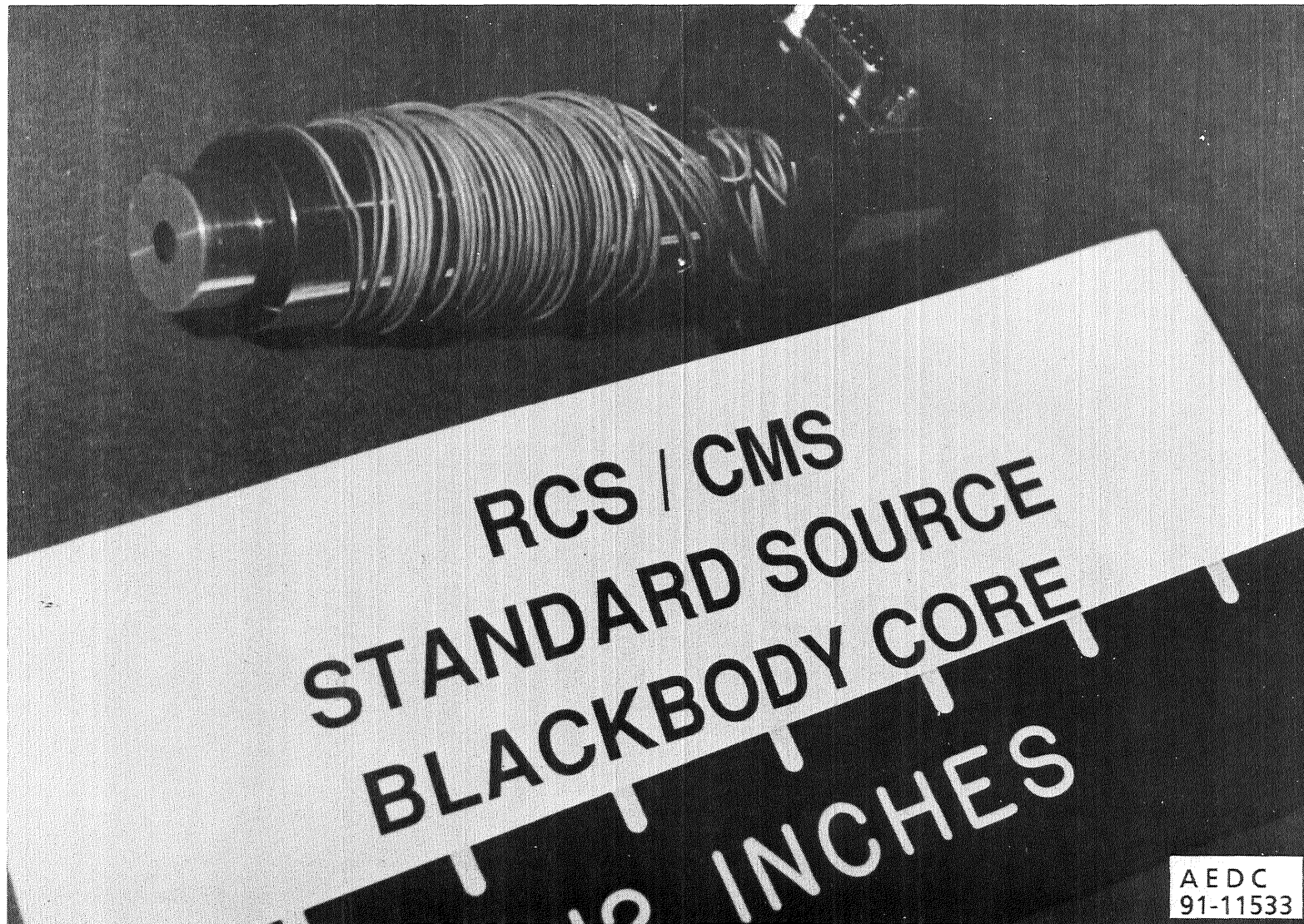


Figure 4. SIRS III blackbody core.

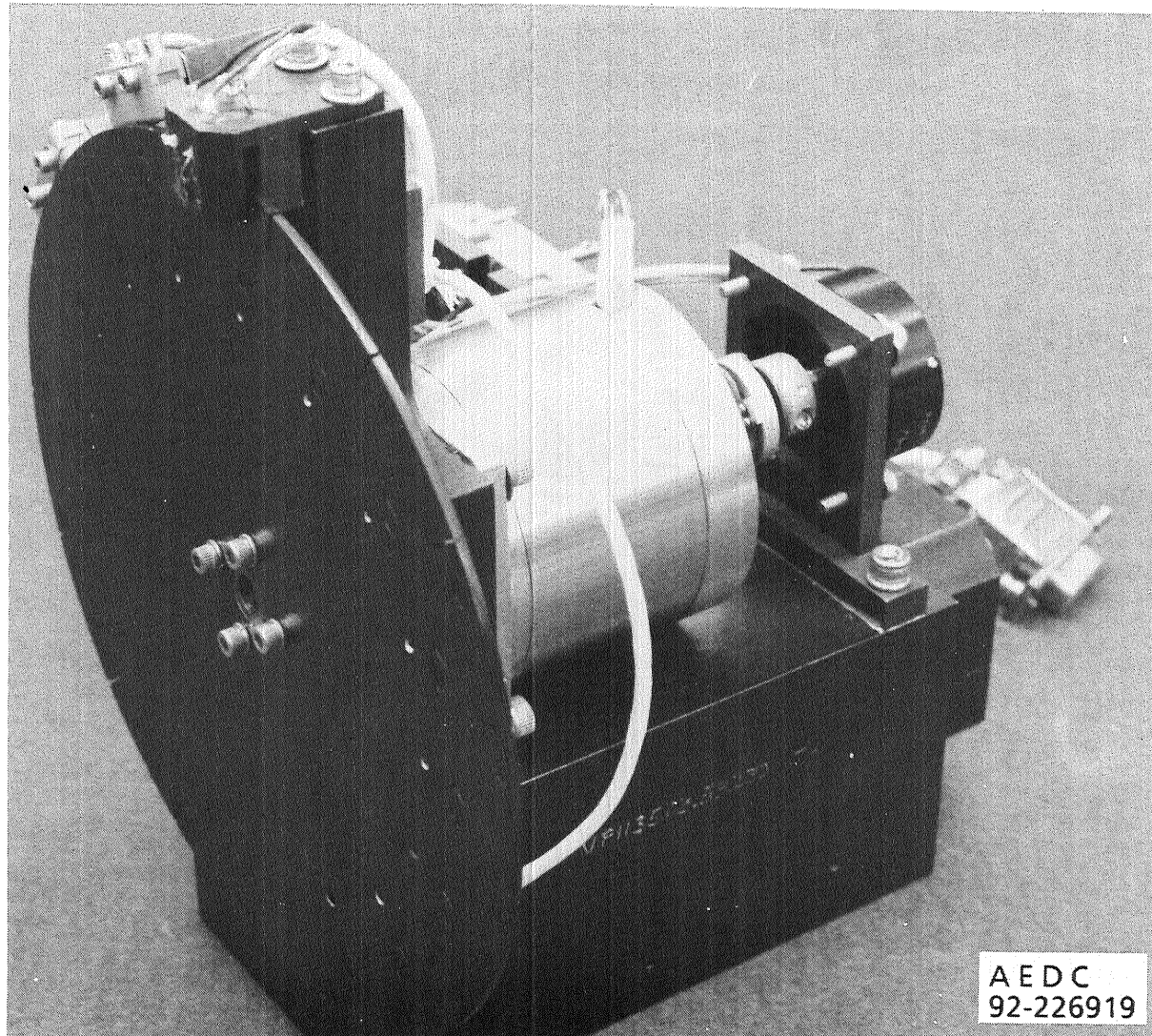


Figure 5. SIRS III assembly.

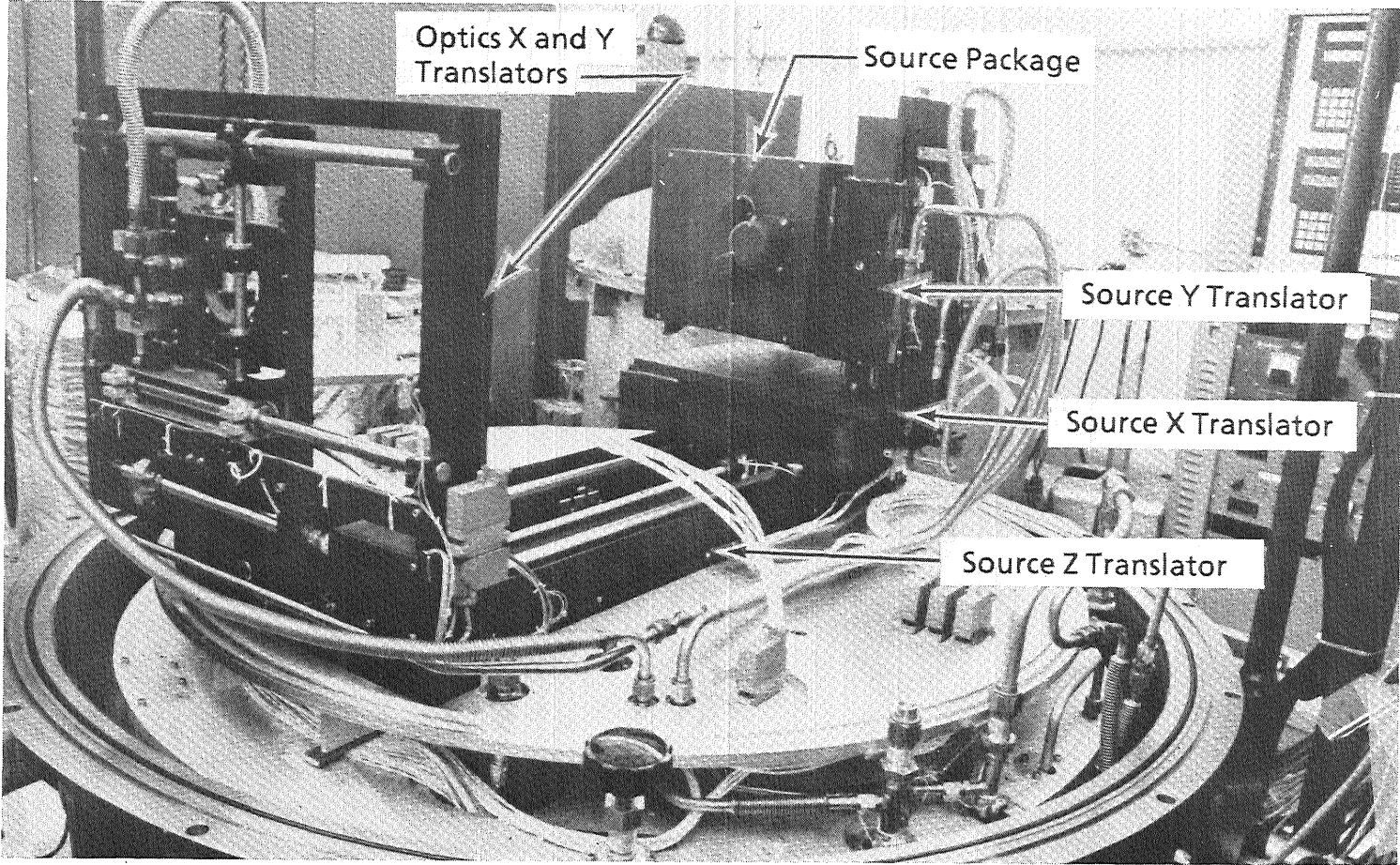


Figure 6. FPCC source package installed in the chamber.

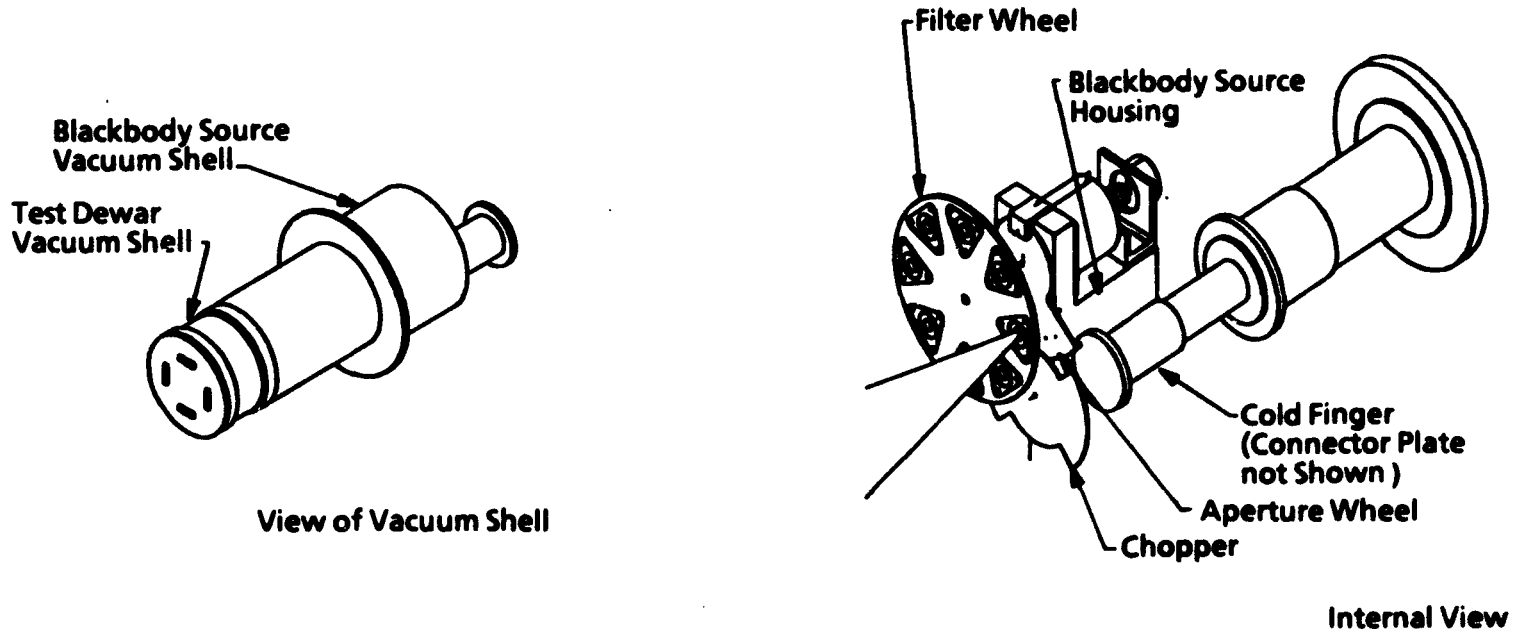
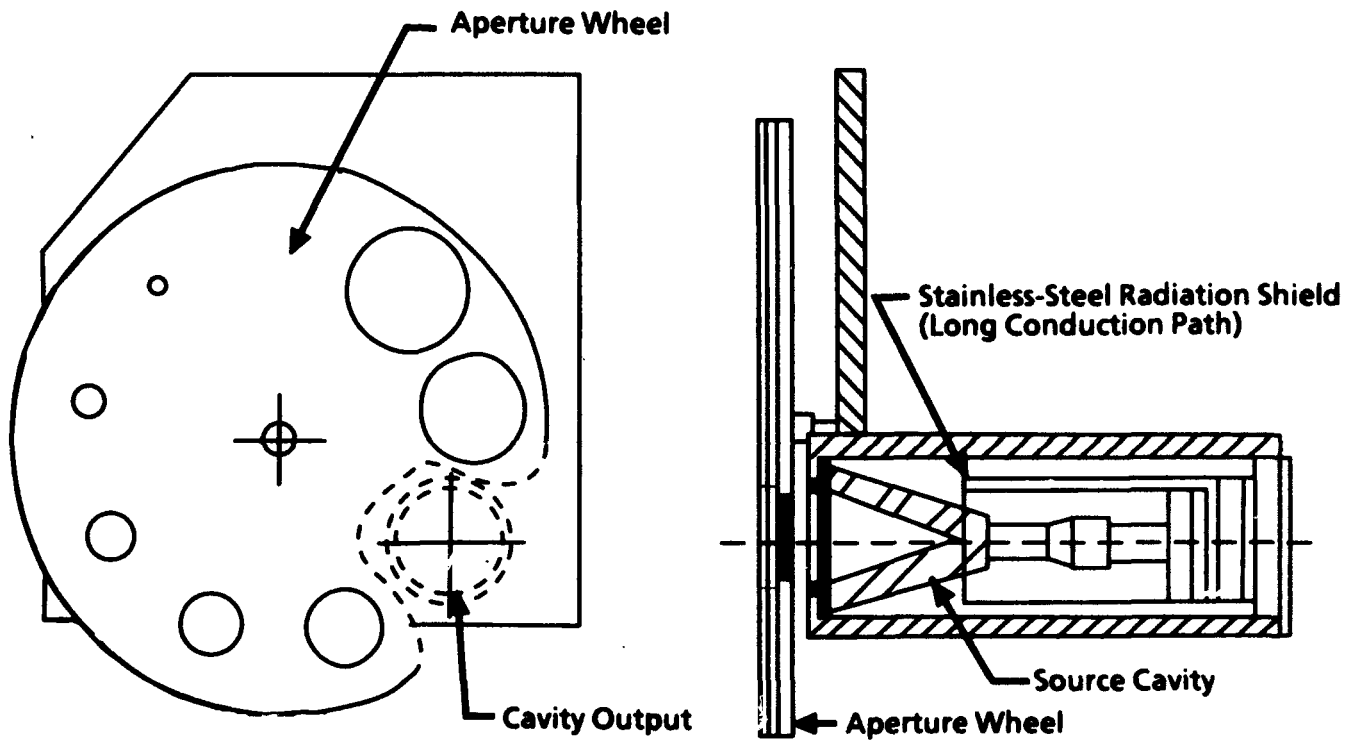


Figure 7. TDWSG source assembly.



**Figure 8. Variable Aperture Blackbody Source (VABS) assembly.**

Cross-Sectional View

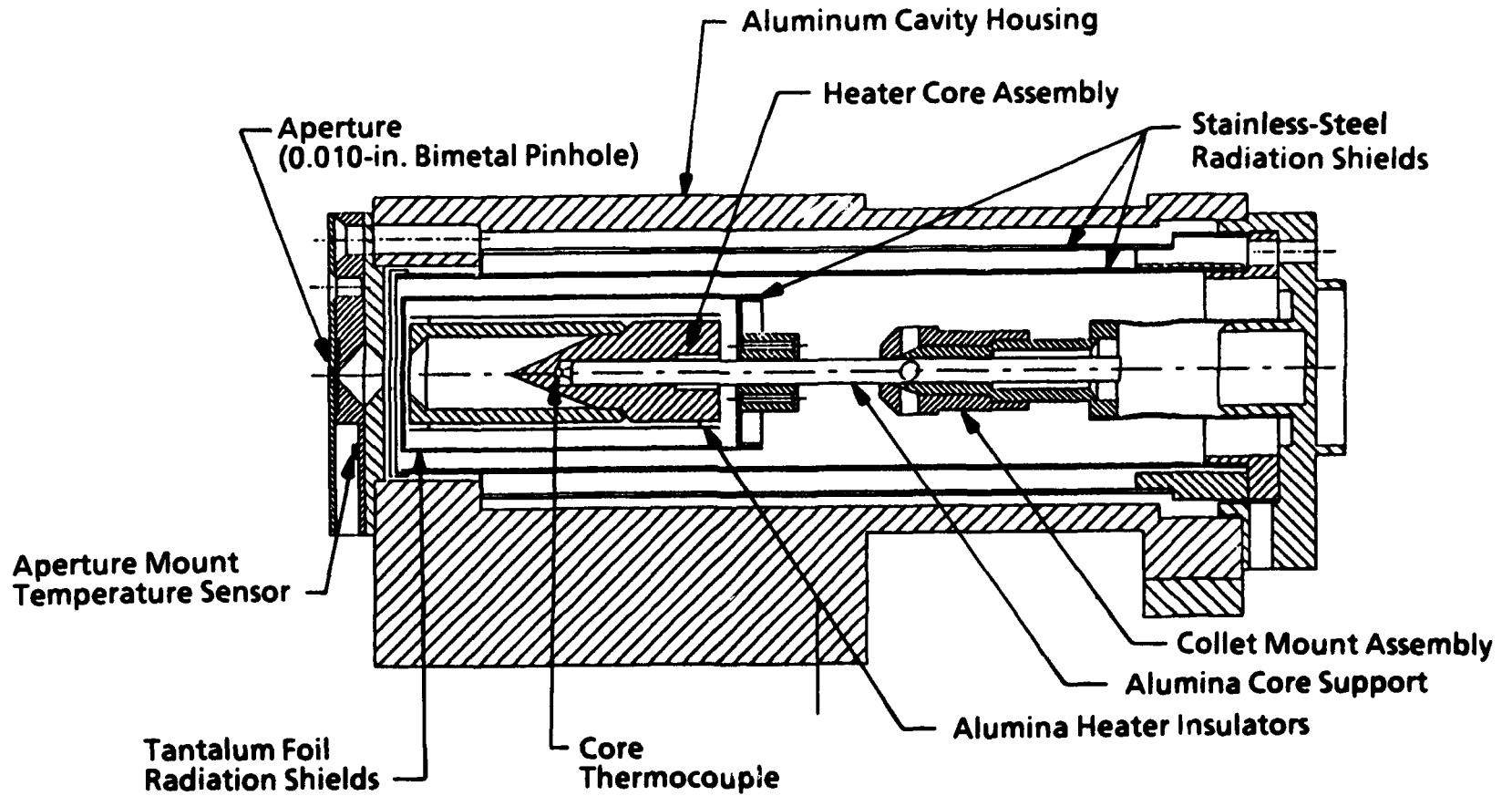


Figure 9. SWIR (1200) blackbody source.

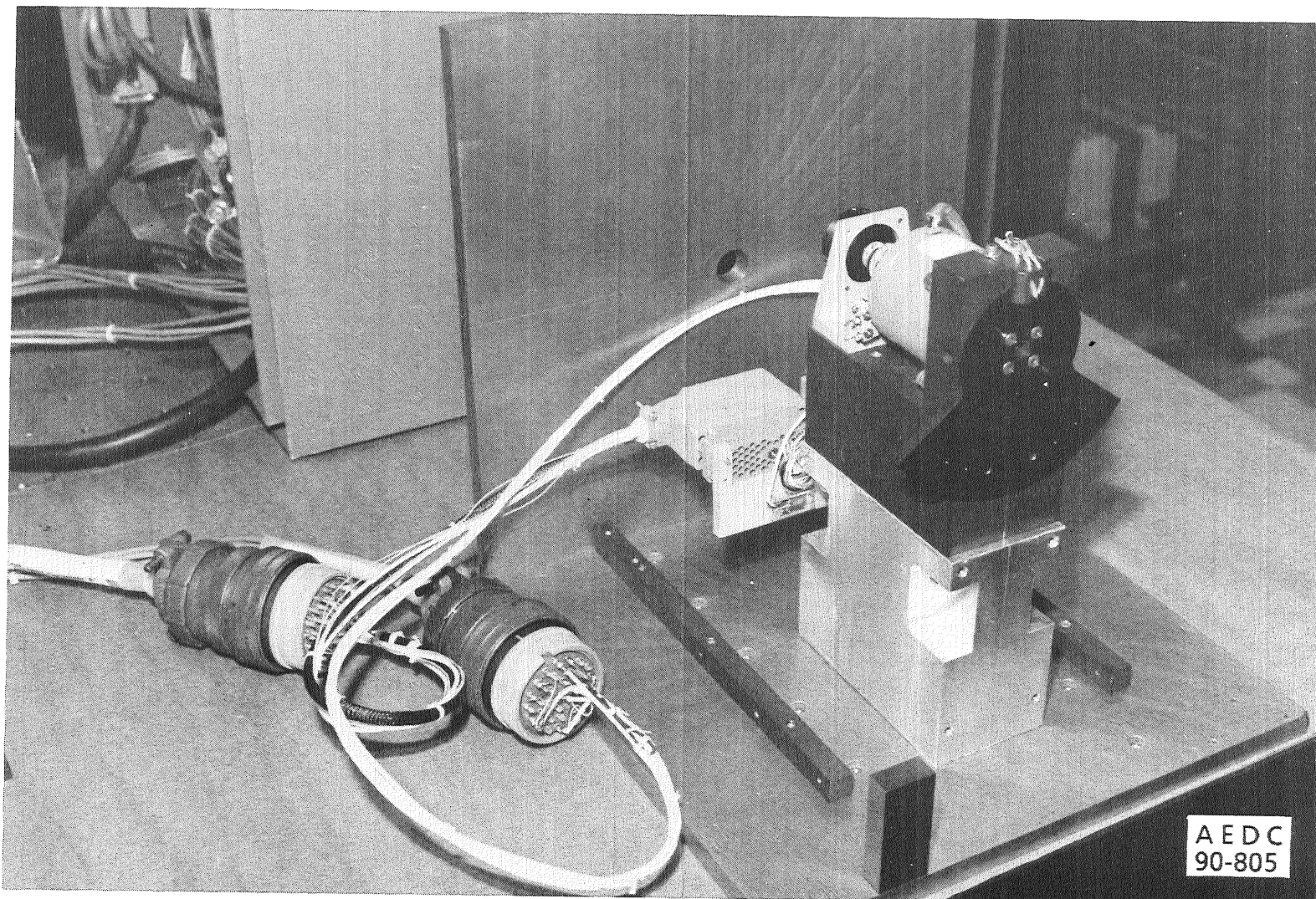


Figure 10. SIRS IIA installation on NIST mounting plate.

- Source ID  
1. SIRS IIB  
2. SIRS IIA  
3. SWIR

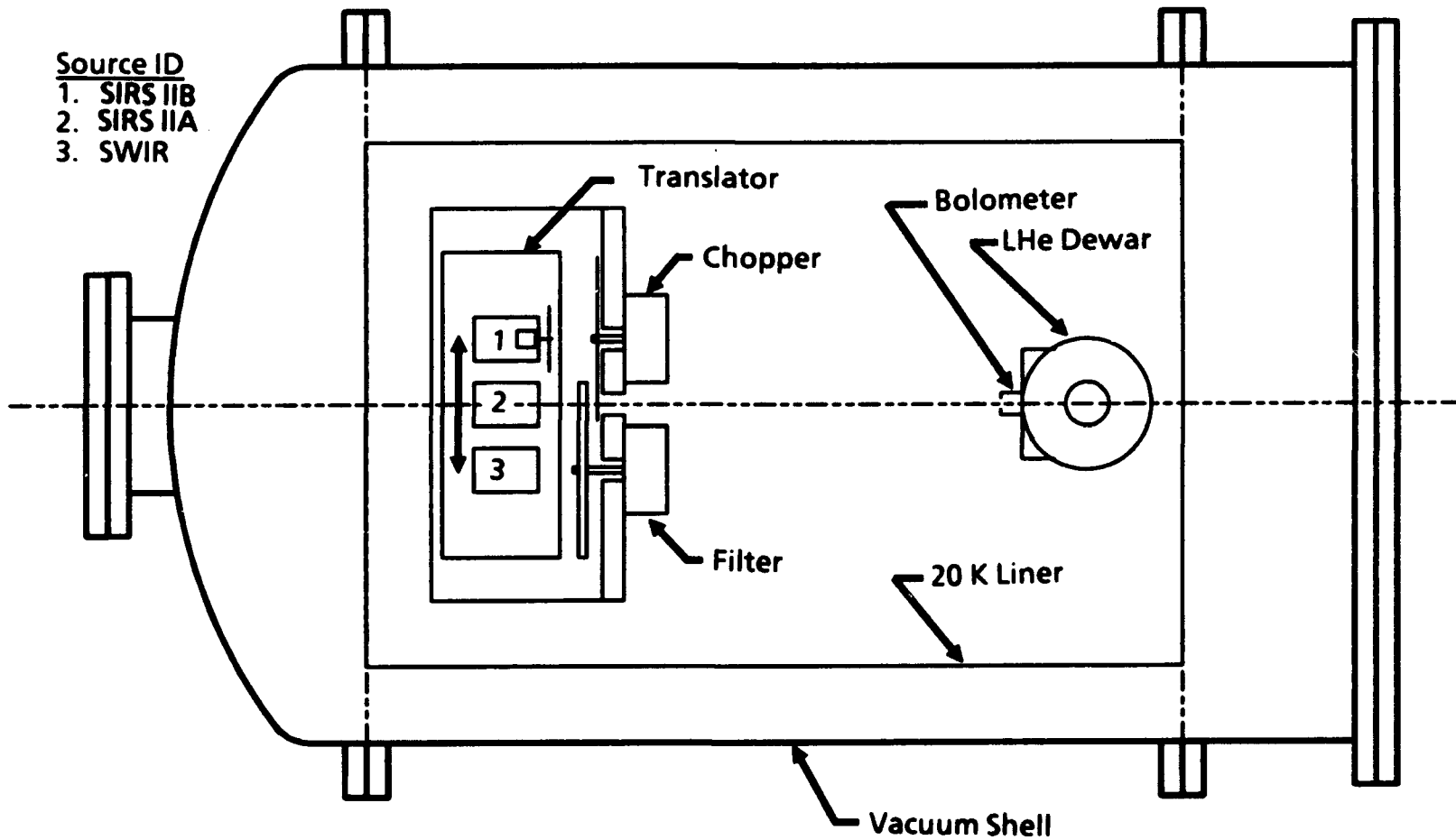


Figure 11. Hardware installation in the UHV Chamber.

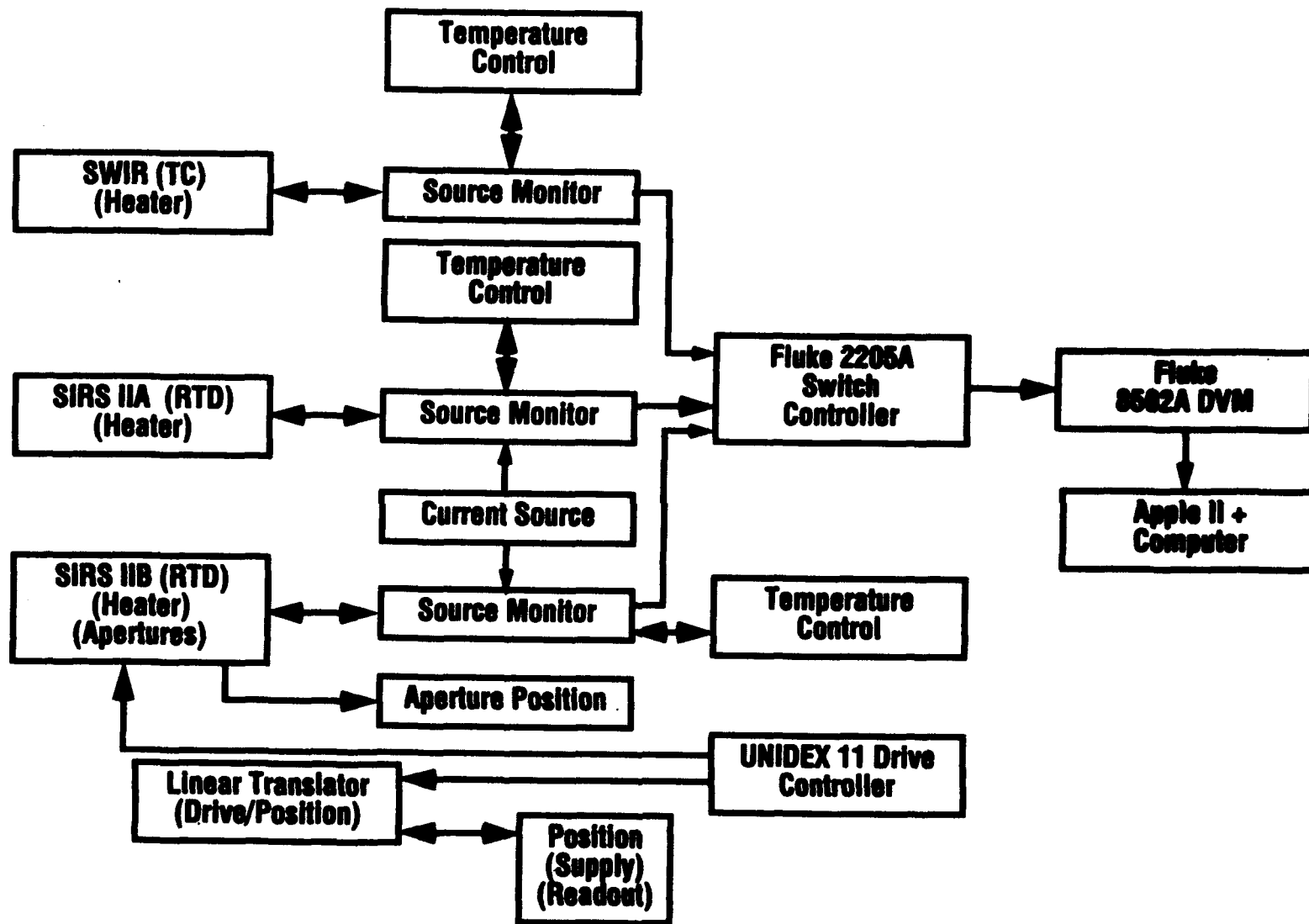


Figure 12. UHV source data acquisition and control system.

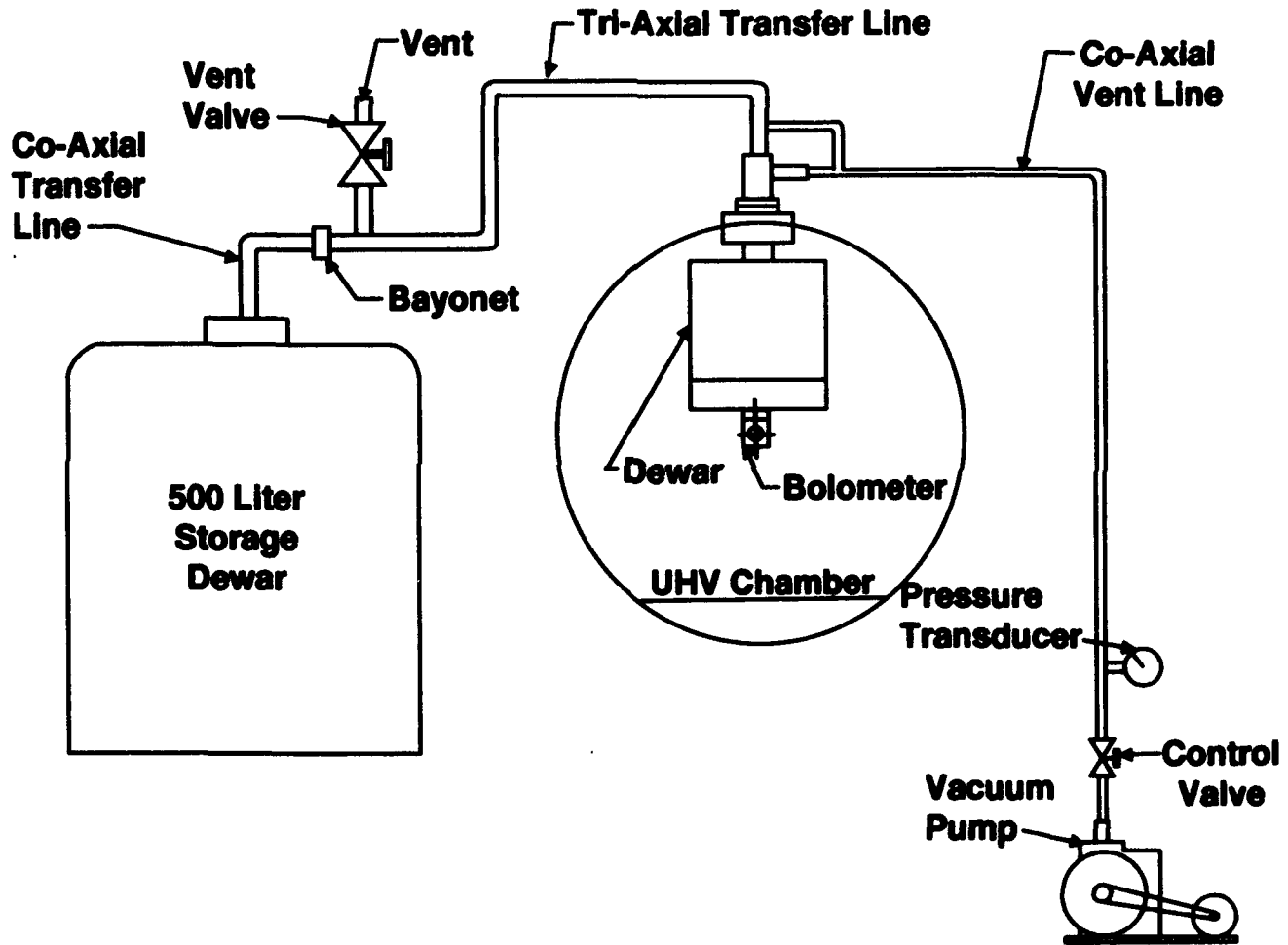


Figure 13. Bolometer dewar system schematic.

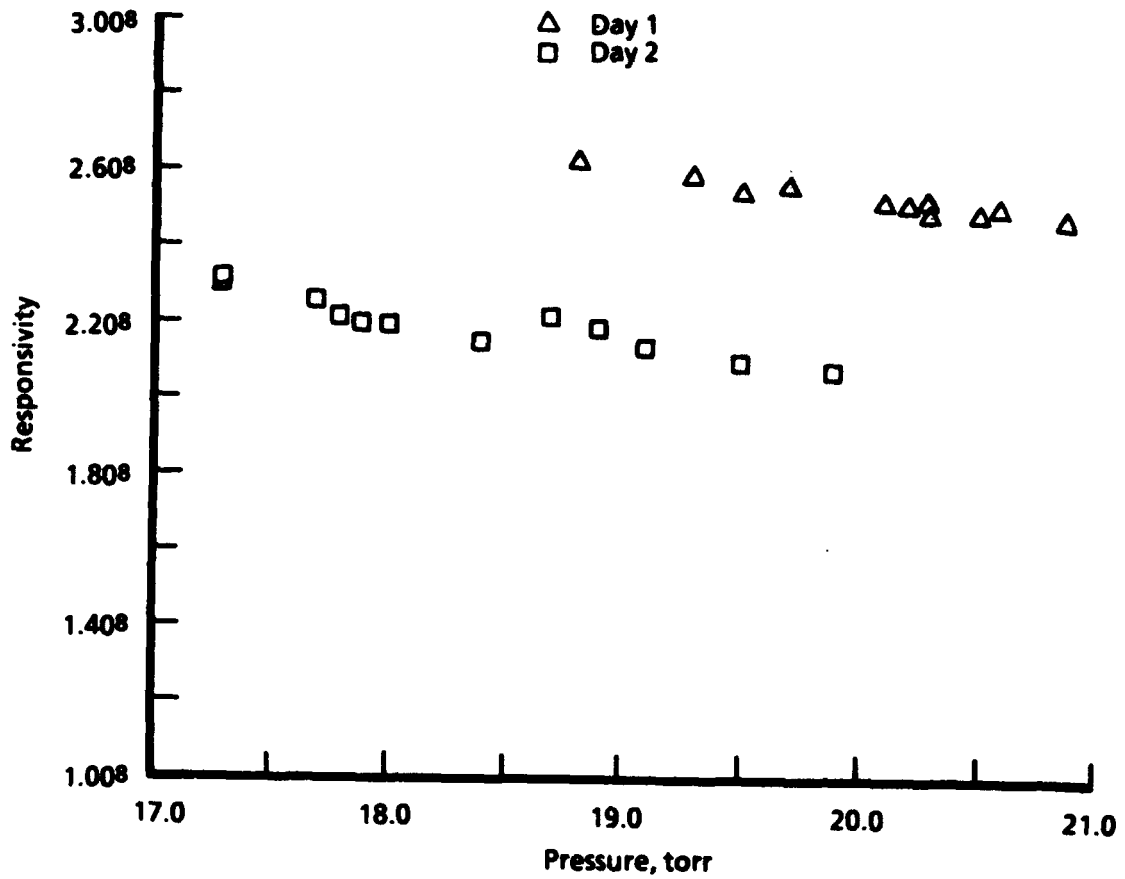


Figure 14. Bolometer responsivity versus dewar pressure.

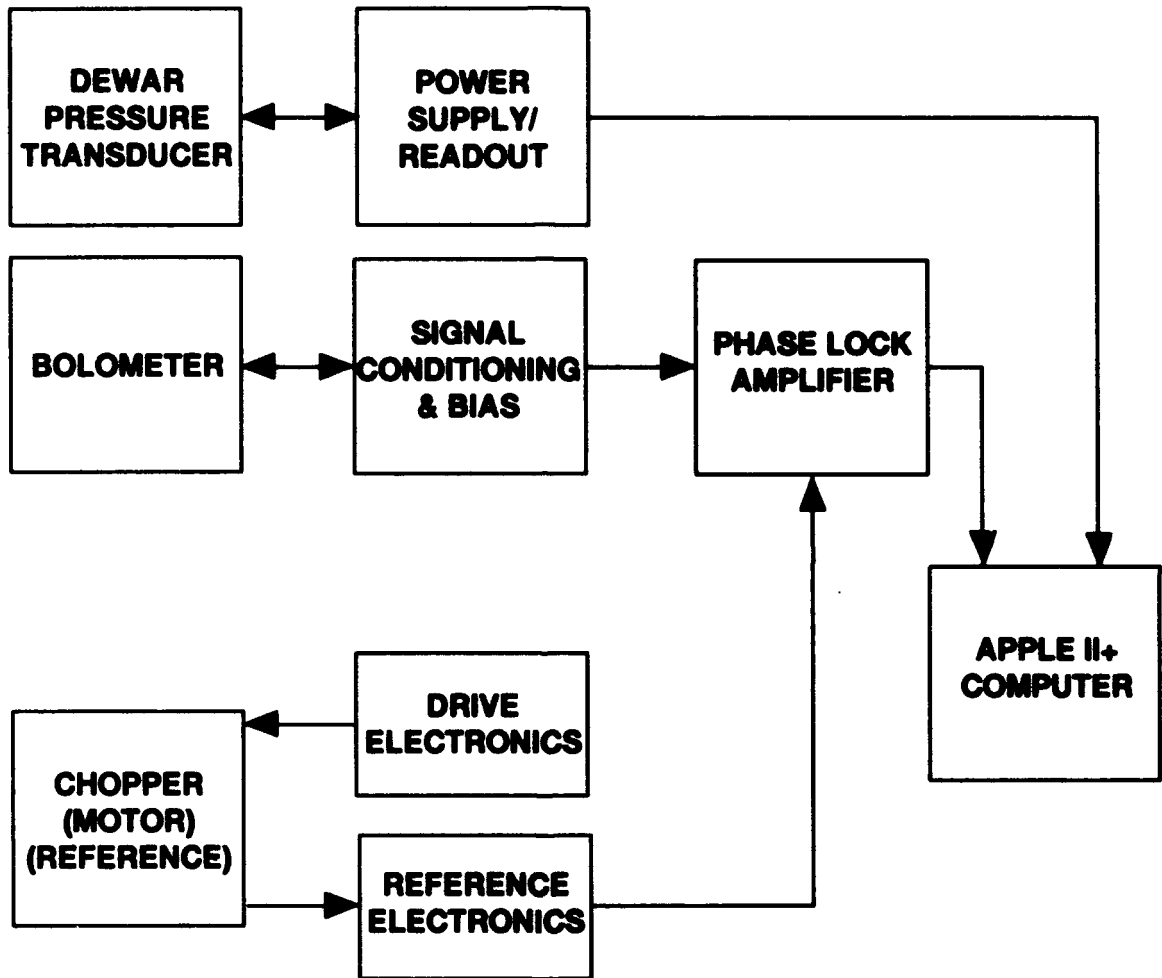


Figure 15. Bolometer instrumentation.

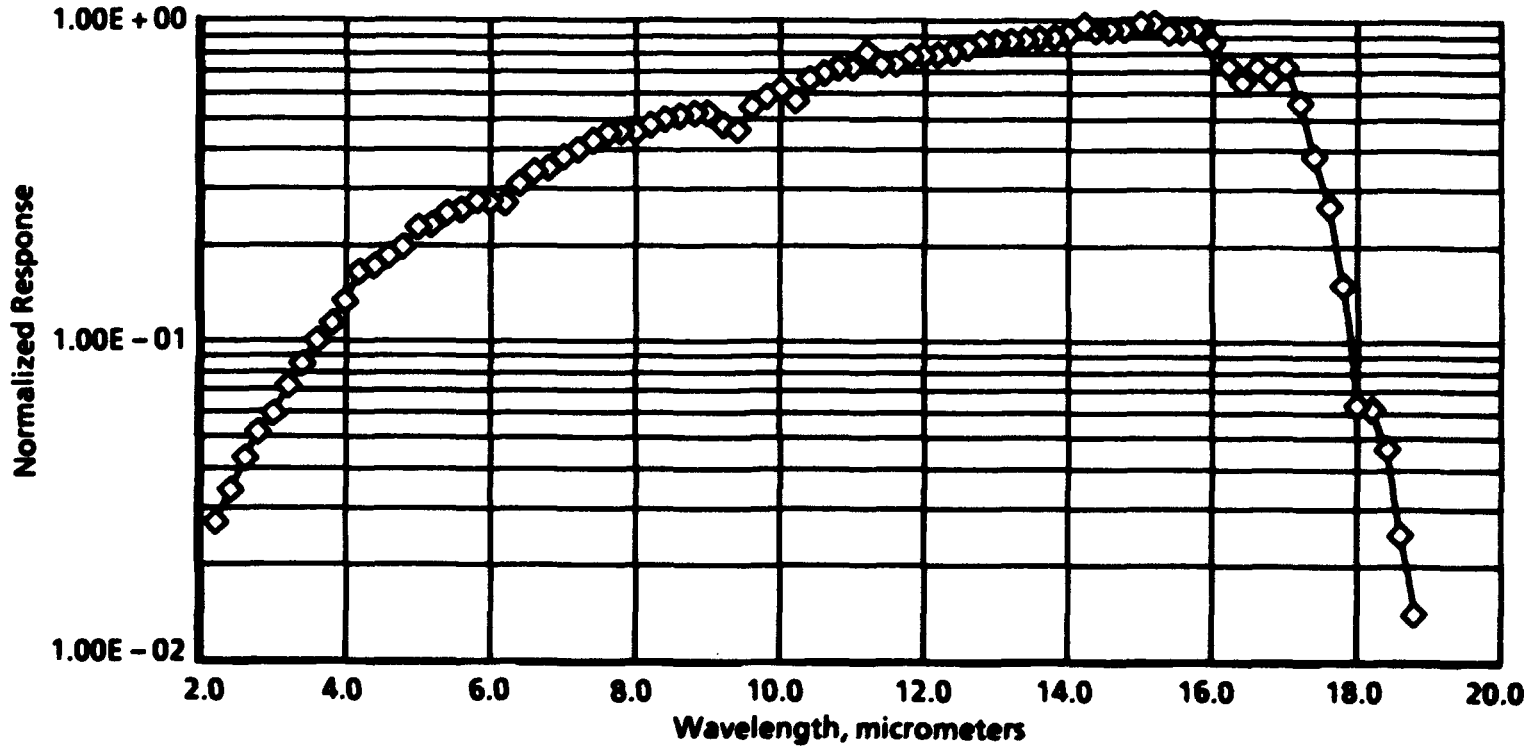


Figure 16. Si:Ga detector normalized spectral response.

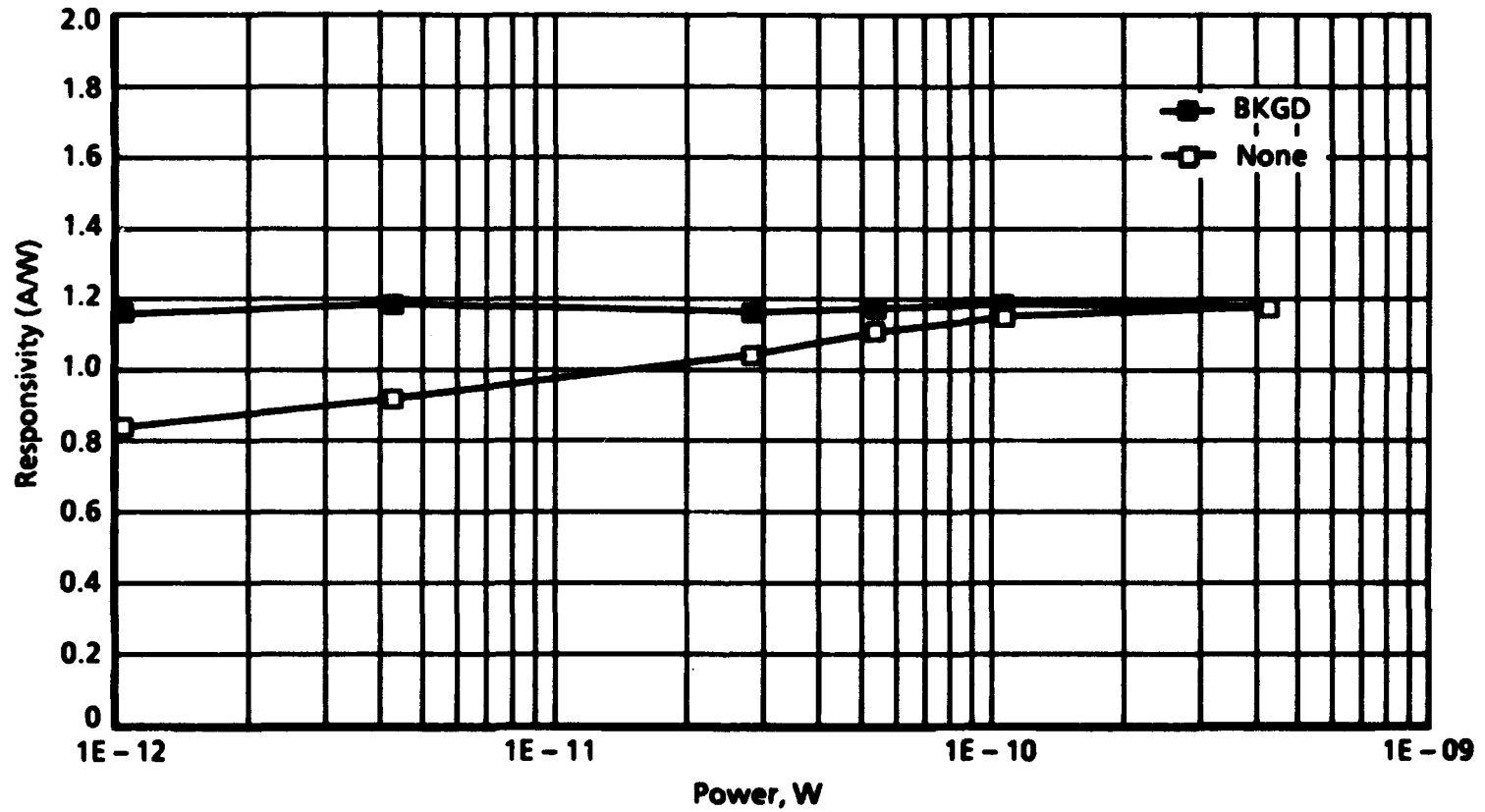


Figure 17. Si:Ga detector responsivity versus power.

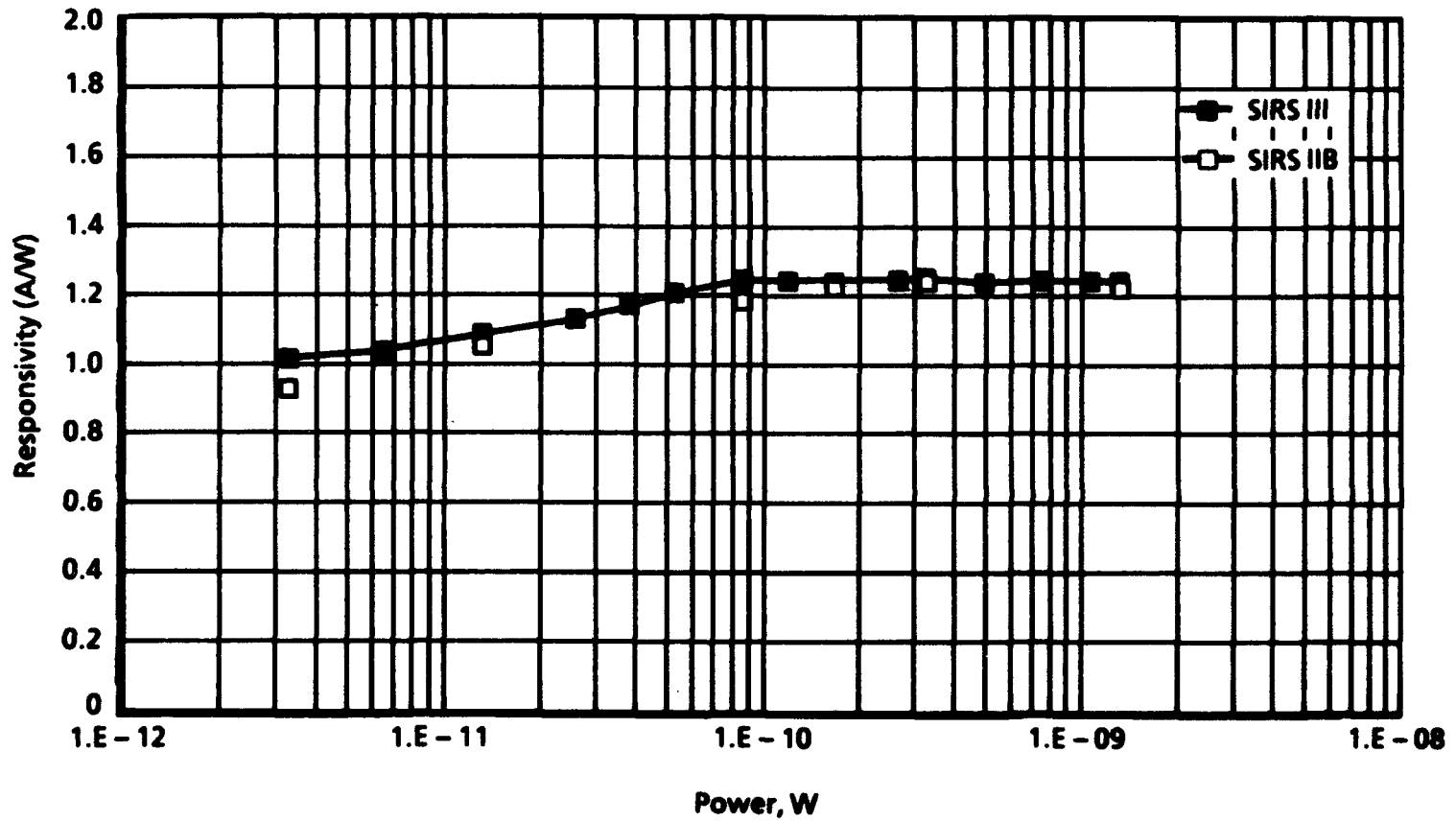


Figure 18. SIRS III transfer calibration results, January 1992.

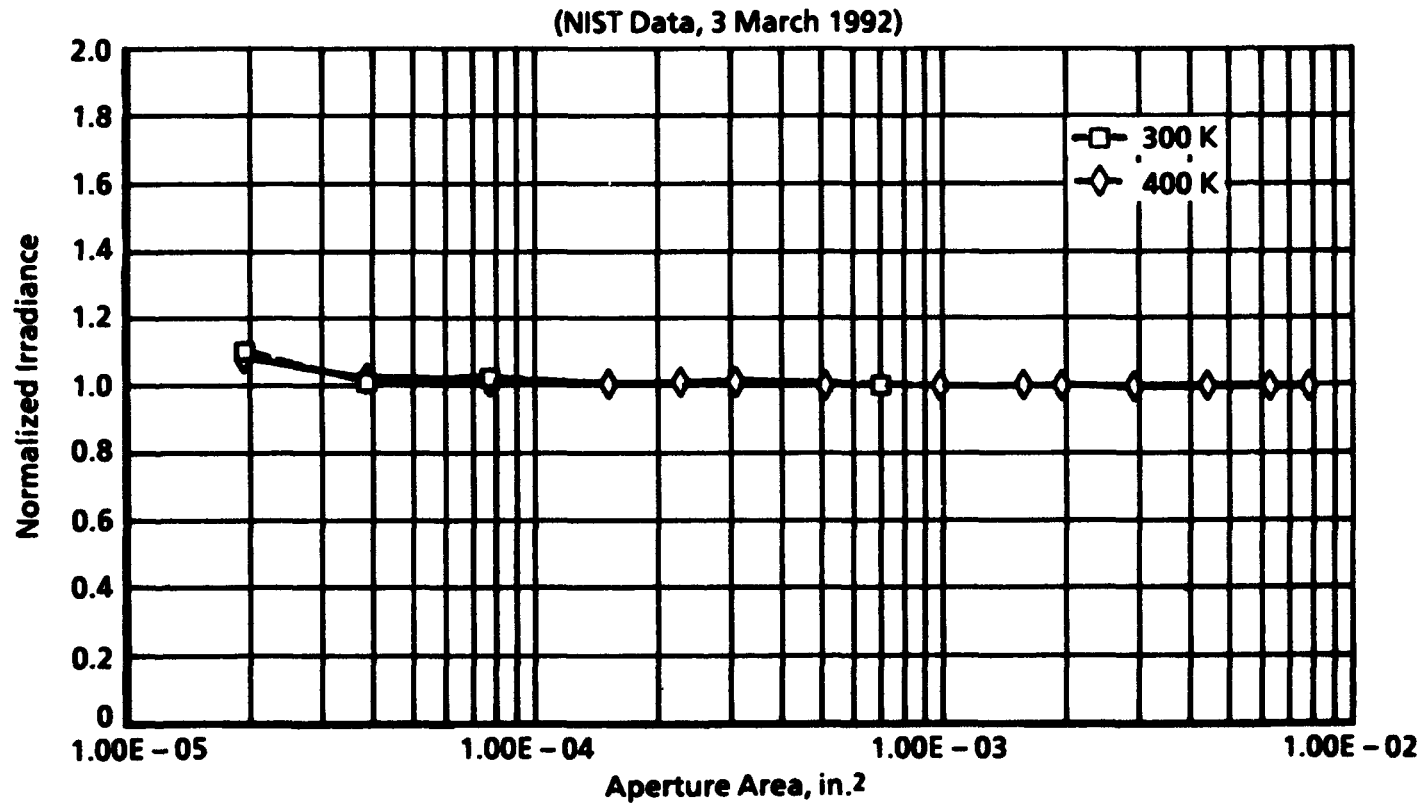


Figure 19. SIRS III output linearity.

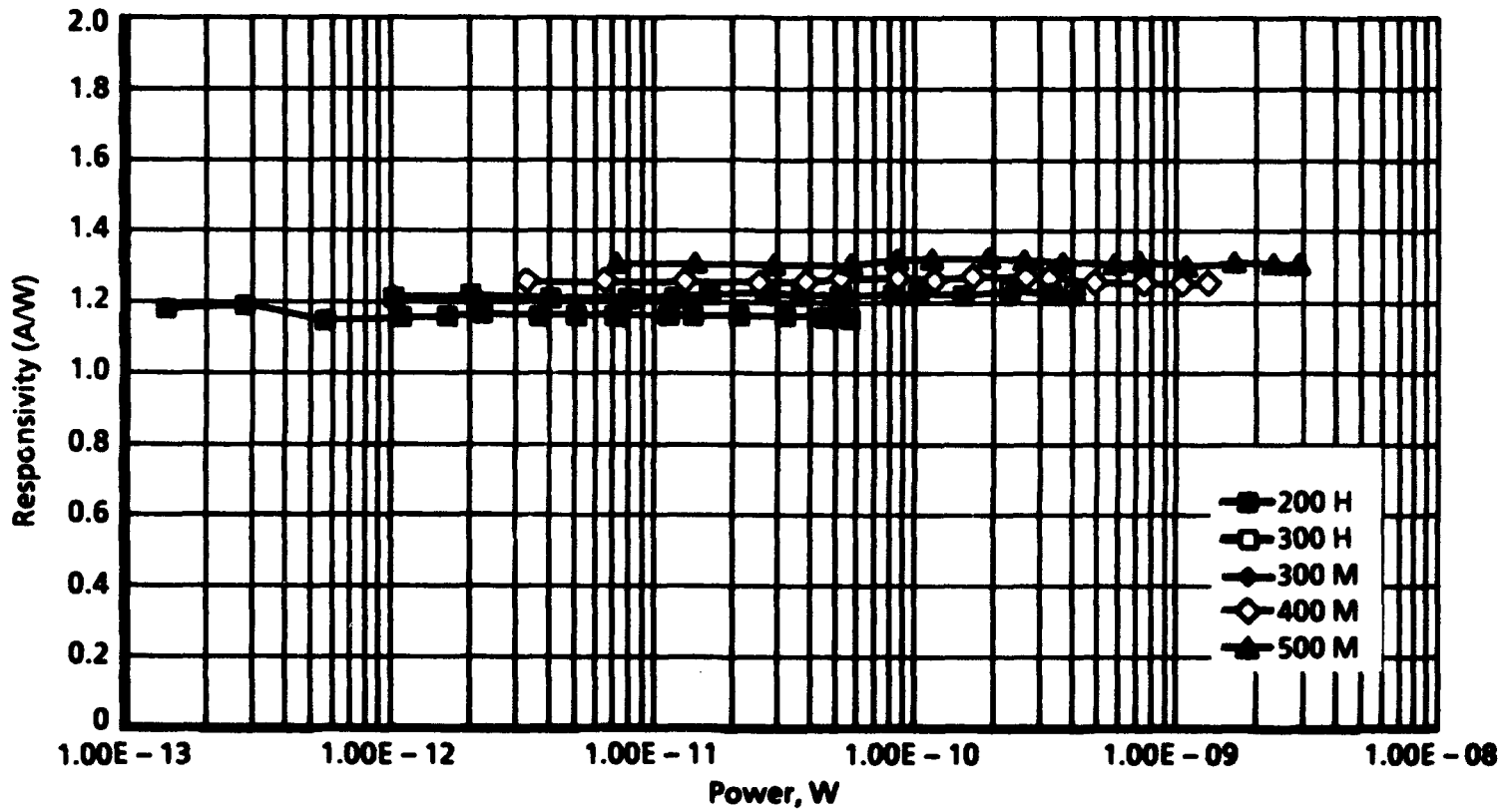


Figure 20. SIRS III source evaluation, June 1992.

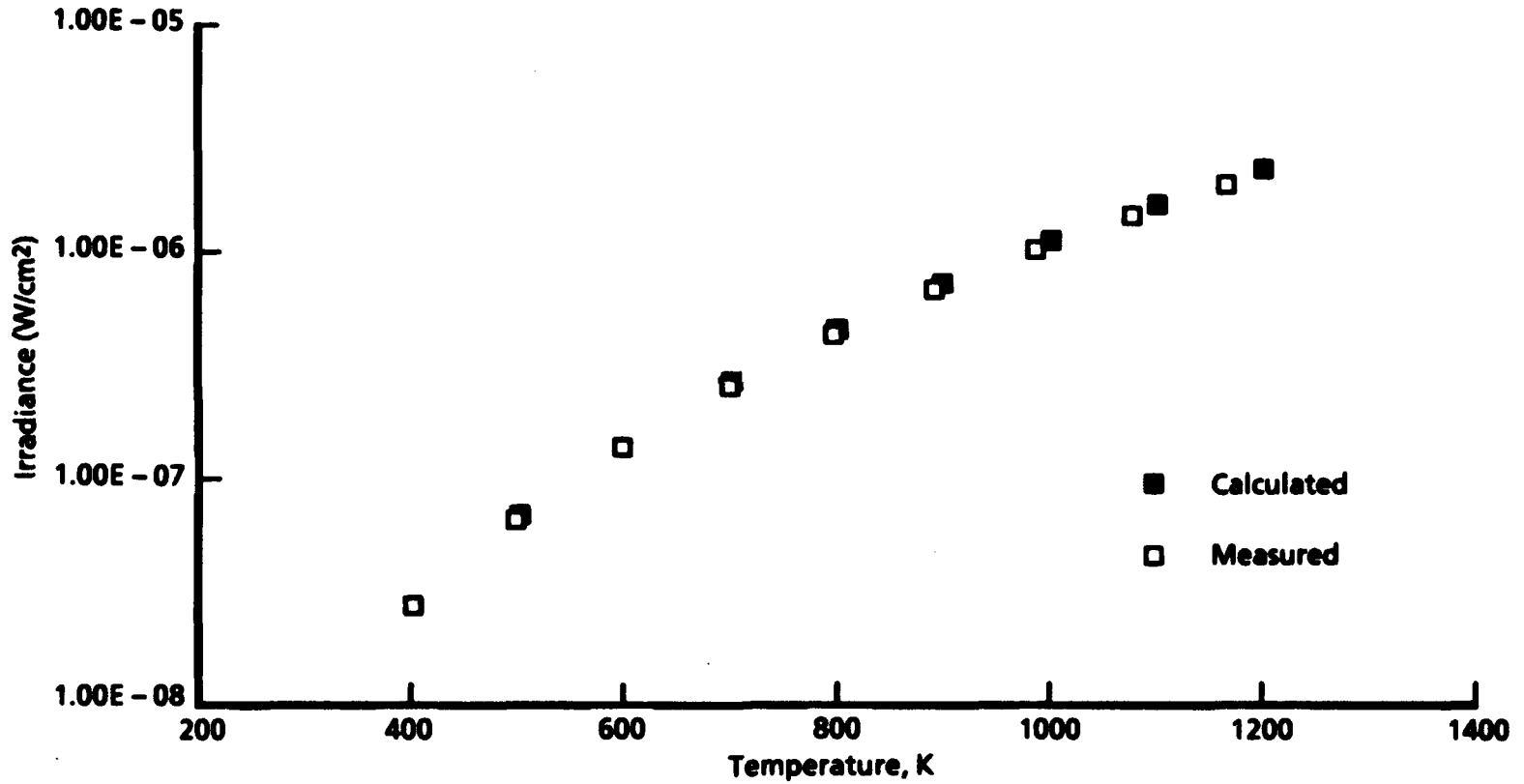


Figure 21. SWIR source output versus cavity temperature.

**Table 1. SIRS IIA Output Aperture Diameters (Inches)**

<b>Wheel Position</b>	<b>Nominal Ambient</b>	<b>Measured</b>	<b>20 K</b>
1	0.0050	0.004933	0.004922
2	0.0100	0.009987	0.009964
3	0.1000	0.100053	0.099823
4	Blank	Blank	Blank
5	0.0500	0.050043	0.049928
6	0.0355	0.035510	0.035428
7	0.0256	0.025600	0.025541

**Table 2. SIRS IIB Output Aperture Diameters (Inches)**

<b>Wheel Position</b>	<b>Nominal Ambient</b>	<b>Measured</b>	<b>20 K</b>
1	0.0050	0.004917	0.004905
2	0.0100	0.010053	0.010030
3	0.1000	0.100080	0.099850
4	Blank	Blank	Blank
5	0.0500	0.049960	0.049845
6	0.0355	0.035533	0.035451
7	0.0256	0.025570	0.025511

**Table 3. SIRS III Output Aperture Diameters (Inches)**

<b>Wheel Position</b>	<b>Measured</b>	<b>20 K</b>
1	Blank	Blank
2	0.004997	0.004985
3	0.007037	0.007020
4	0.009987	0.009964
5	0.013967	0.013934
6	0.010866	0.010841
7	0.019967	0.019921
8	0.025617	0.025558
9	0.029977	0.029908
10	0.035533	0.035452
11	0.044833	0.044730
12	0.049947	0.049832
13	0.061113	0.060973
14	0.075260	0.075087
15	0.089567	0.089361
16	0.100013	0.099783

**Table 4. FPCC Source Output Aperture Diameters (Inches)**

<b>Aperture Number</b>	<b>Measured</b>
1	0.012726
2	0.025545
3	0.253848
4	Blank
5	0.127012
6	0.090002
7	0.064879

**Table 5. TDWSG Source Output Aperture Diameters (Inches)**

<b>Aperture Position</b>	<b>Nominal</b>	<b>Measured</b>
1	0.005	0.04917
2	0.010	0.01005
3	0.100	0.10008
4	Blank	Blank
5	0.050	0.04996
6	0.0355	0.03553
7	0.0256	0.02557

**Table 6. VABS Output Aperture Diamters (Inches)**

Aperture Number	Measured	20 K
1	Blank	Blank
2	0.0298	0.0297
3	0.0498	0.0496
4	0.1048	0.1044
5	0.2092	0.2083
6	0.3662	0.3647
7	0.5232	0.5210
8	0.7322	0.7292
9	1.0002	0.9960

**Table 7. FY90 SIRS IIA Calibration Equations and Coefficients**

Aperture Number	Sensor A		Sensor B	
	A <sub>0</sub>	A <sub>1</sub>	A <sub>0</sub>	A <sub>1</sub>
2	0	1.0122	0	1.0118
3	-1.13	1.0072	0.28	1.0029
5	-1.74	1.0120	-0.20	1.0074
6	-1.62	1.0107	0	1.00587
7	-0.61	1.006	0	1.0046

$$T_R = A_0 + A_1(T_M)$$

Table 8. FY90 SIRS IIA Calibration Data - Sensor A Aperture 3

Sensor A Data, K	Mean Radiance Temperature, K	Radiance Deviation, percent	Total Radiance Uncertainty, percent
100.039	99.6	-1.775	2.8
150.007	150.0	-0.019	1.6
199.893	200.2	0.612	1.2
224.750	225.2	0.797	1.2
249.683	250.4	1.140	1.2
274.686	275.5	1.177	0.8
299.544	300.6	1.398	0.8
324.421	325.6	1.441	0.8
349.360	350.7	1.520	0.8
374.093	375.7	1.700	0.8
399.077	400.3	1.216	0.8

**Table 9. FY90 and FY93 SIRS IIA Diffraction Correction Percentages**

Nominal Blackbody Temp, K	Aperture Nos.					
	1	2	3	5	6	7
100	18.1	7.8	± 1.2	1.7	1.9	2.7
125	13.9	6.2	± 1.0	1.5	1.5	2.2
150	11.3	5.1	± 0.8	1.3	1.3	1.8
175	9.6	4.3	± 0.7	1.1	1.1	1.5
200	8.3	3.8	± 0.6	1.0	1.0	1.3
225	7.3	3.3	± 0.5	0.9	0.9	1.2
250	6.5	3.0	± 0.5	0.8	0.8	1.1
275	5.9	2.7	± 0.4	0.7	0.7	1.0
300	5.4	2.5	± 0.4)	0.6	0.6	0.9
325	4.9	2.3	± 0.4	0.6	0.6	0.8
350	4.6	2.1	± 0.4	0.5	0.5	0.8
375	4.2	2.0	± 0.4	0.5	0.5	0.7
400	3.6	1.9	± 0.4	0.5	0.5	0.7

**Table 10. FY93 SIRS IIA Calibration Equations and Coefficients**

Aperture Number	Sensor A		Sensor B	
	A <sub>0</sub>	A <sub>1</sub>	A <sub>0</sub>	A <sub>1</sub>
1	0	1.0046	0	1.0041
2	0	1.0094	0	1.0089
3	0	1.0073	1.34	1.0034
5	0	1.007	1.34	1.003
6	0	1.005	1.25	1.0012
7	0	1.0025	0.95	1.00

$$T_R = A_0 + A_1 (T_M)$$

**Table 11. FY93 SIRS IIA Calibration Data**

Sensor A Data, K	Radiance Temperature, K	Radiance Deviation, percent	Total Radiance Uncertainty, percent
100.00	100.73	2.87	0.4
150.00	151.10	2.88	0.4
200.00	201.46	2.87	0.4
250.00	251.83	2.88	0.4
300.00	302.19	2.87	0.4
350.00	352.56	2.87	0.4
400.00	402.93	2.88	0.4

**Table 12. FY90 and FY93 SIRS IIA Calibration Coefficient Comparison (Temperature Sensor A)**

Aperture Number	A <sub>0</sub>		A <sub>1</sub>	
	90	93	90	93
1	---	0.0	---	1.0046
2	0.0	0.0	1.0122	1.0094
3	-1.1	0.0	1.0072	1.0073
5	-1.7	0.0	1.0120	1.0070
6	-1.6	0.0	1.0107	1.0050
7	-0.6	0.0	1.0060	1.0025

$$T_R = A_0 + A_1 (T_M)$$

**Table 13. FY90 and FY93 SIRS IIA NIST Calibration Results Comparison (Aperture No. 3)**

Nominal Temp, K	Temperature Diff, percent		Radiometric Diff, percent	
	May 90	April 93	May 90	April 93
100	0.9	1.1	3.7	4.5
150	0.3	0.9	1.3	3.8
200	0.2	1.1	0.8	4.3
300	0.3	0.7	1.3	3.0
400	0.5	0.7	1.8	3.0
<b>Average</b>	<b>0.4</b>	<b>0.9</b>	<b>1.8</b>	<b>3.7</b>

**Table 14. FY92 SIRS III Calibration Equations  
and Coefficients - Sensor A**

Aperture Number	Coefficients	
	A <sub>0</sub>	A <sub>1</sub>
2	4.3197	1.0191
3	0	1.0154
4	1.1605	1.0089
5	-1.3627	1.0110
6	-2.909	1.0154
7	-1.0005	1.0127
8	-0.9253	1.0110
9	-1.3677	1.0110
10	-1.6200	1.0105
11	-1.2499	1.0106
12	-1.1083	1.0100
13	-1.0974	1.0081
14	-1.083	1.0092
15	-1.0846	1.0086
16	-0.9867	1.0090

$$T_R = A_0 + A_1 (T_M)$$

**Table 15. FY92 SIRS III Calibration Data - Sensor A Aperture 16**

<b>Sensor A Temp, K</b>	<b>Radiance Temp, K</b>	<b>Radiance Deviation, percent</b>	<b>Total Radiance Uncertainty, percent</b>
<b>200</b>	<b>200.82</b>	<b>1.623</b>	<b>0.48</b>
<b>250</b>	<b>251.26</b>	<b>1.991</b>	<b>0.44</b>
<b>300</b>	<b>301.71</b>	<b>2.248</b>	<b>0.40</b>
<b>350</b>	<b>352.16</b>	<b>2.431</b>	<b>0.36</b>
<b>400</b>	<b>402.61</b>	<b>2.568</b>	<b>0.36</b>
<b>450</b>	<b>453.06</b>	<b>2.674</b>	<b>0.36</b>
<b>500</b>	<b>503.50</b>	<b>2.752</b>	<b>0.36</b>

**Table 16. FY92 SIRS III Diffraction Correction Percentages**

Nominal Blackbody Temp, K	Aperture Nos.														
	2	3	4	5	6	7	8	9	10	11	12	13	14	15	16
200	1.8	0.9	0.3	-0.1	-0.3	-0.3	-0.3	-0.3	-0.3	-0.3	-0.3	-0.3	-0.3	-0.3	-0.3
250	1.3	0.8	0.2	0	-0.2	-0.3	-0.3	-0.3	-0.3	-0.3	-0.3	-0.3	-0.1	-0.2	-0.2
300	1.2	0.6	0.2	0	-0.2	-0.3	-0.3	-0.3	-0.3	-0.2	-0.2	-0.2	-0.1	-0.2	-0.2
350	1.0	0.5	0.2	0	-0.1	-0.2	-0.2	-0.2	-0.2	-0.2	-0.2	-0.2	-0.1	-0.2	-0.1
400	0.9	0.4	0.1	0	-0.1	-0.2	-0.2	-0.2	-0.2	-0.2	-0.2	-0.2	-0.1	-0.1	-0.1
450	0.7	0.4	0.1	0	-0.1	-0.2	-0.1	-0.1	-0.1	-0.1	-0.1	-0.1	-0.1	-0.1	-0.1
500	0.7	0.4	0.1	0	-0.1	-0.1	-0.1	-0.1	-0.1	-0.1	-0.1	-0.1	-0.1	-0.1	-0.1

**Table 17. SIRS IIA and SIRS IIB Comparison Summary  
(Si:Ga, 12 V Bias, 14.9 K, 4/29/92)**

Source Temp, K	TIA Gain	Detector Responsivity (A/W)		Deviation, percent
		SIRS IIA	SIRS IIB	
200	H	1.10	1.05	4.5
300	H	1.15	1.13	1.7
300	M	1.14	1.13	0.9
300	M	1.15	1.13	1.7
300	H	1.14	1.13	0.9
400	M	1.18	1.19	0.8
500	M	---	1.23	---

SIRS IIA 6 Apertures  
SIRS IIB 6 Apertures

**Table 18. SIRS IIA and SIRS III Comparison Summary  
(Si:Ga, 12 V Bias, 17.9 K, 6/24/92)**

Source Temp, K	TIA Gain	Detector Responsivity (A/W)		Deviation, percent
		SIRS IIA	SIRS III	
200	H	1.14	1.16	1.8
300	H	1.19	1.22	2.5
300	M	1.19	1.21	1.7
400	M	1.24	1.26	1.6
500	M	---	1.31	---

SIRS IIA 6 Apertures  
SIRS III 16 Apertures

**Table 19. SIRS IIA and TDWSG Comparison Summary  
(Si:Ga, 12 V Bias, 15 K, 9/9/92)**

Source Temp, K	TIA Gain	Detector SIRS IIA	Responsivity (A/W) TDWSG	$\Delta$ , percent	Deviation, percent
300	H	1.14	1.20	---	5.2
300	M	1.13	1.19	---	5.3
400	M	1.19	1.26	5.5	5.9
493	M	---	1.30	3.1	---
595	M	---	1.35	3.7	---
696	M	---	1.41	4.3	---
696	L	---	1.38	---	---
792	L	---	1.41	---	---

$$\Delta = \frac{R_{n+1} - R_n}{R_{n+1}} (100\%)$$

Table 20. SIRS IIA and VABS Comparison Summary

Data Set	Temp, K	Bolometer Responsivity (mV/QW)		Deviation, percent
		SIRS IIA	VABS	
1	200	3.23E10	3.25E10	0.54
2	250	3.62E10	3.53E10	-2.70
3	250	3.31E10	3.27E10	-1.18
4	300	3.48E10	3.49E10	0.51
5	300	3.48E10	3.46E10	-0.51
6	300	2.28E10	2.28E10	-0.10
7	350	3.46E10	3.42E10	-0.91
8	350	3.21E10	3.18E10	-0.84
9	400	3.40E10	3.36E10	-1.11
10	400	3.18E10	3.15E10	-0.82
				Average = -0.71

Table 21. SWIR Source Calibration Results

Run Number	T, K	Calculated Irradiance, W/cm <sup>2</sup>	Measured Irradiance, W/cm <sup>2</sup>	Difference, percent	Calculated T <sub>eff</sub> , K
1	400.2	2.67E - 08	2.73E - 08	- 2.43	402.6
3	502.5	6.73E - 08	6.53E - 08	3.07	498.6
4	598.0	1.36E - 07	1.36E - 07	0.22	599.2
5	701.6	2.60E - 07	2.53E - 07	2.96	699.4
6	800.7	4.44E - 07	4.26E - 07	3.96	797.2
7	901.3	7.16E - 07	6.73E - 07	5.98	893.5
8	1002.7	1.10E - 06	1.01E - 06	8.44	988.3
9	1101.6	1.61E - 06	1.43E - 06	11.08	1078.6
10	1202.1	2.28E - 06	1.96E - 06	14.37	1166.6
11	1102.6	1.61E - 06	1.44E - 06	11.03	1079.7
13	1002.9	1.10E - 06	1.01E - 06	8.14	989.3
14	902.5	7.20E - 07	6.70E - 07	6.88	892.6
15	901.4	4.46E - 07	4.28E - 07	3.86	798.1
17	503.1	6.77E - 08	6.63E - 08	2.05	500.5
18	602.9	1.41E - 07	1.38E - 07	1.97	601.4
19	702.5	2.62E - 07	2.52E - 07	3.85	698.7
20	800.5	4.44E - 07	4.25E - 07	4.18	796.6
22	901.4	7.16E - 07	6.75E - 07	5.70	894.3
23	1003.5	1.10E - 06	1.02E - 06	7.50	991.6
24	1102.4	1.61E - 06	1.44E - 06	10.76	1080.3
25	1202.2	2.29E - 06	1.97E - 06	13.71	1169.0
26	1102.5	1.61E - 06	1.44E - 06	10.81	1080.3
27	1003.7	1.10E - 06	1.03E - 06	6.55	986.8
28	902.4	7.19E - 07	6.84E - 07	4.95	897.0
29	801.1	4.45E - 07	4.24E - 07	4.60	796.2